DIABETES

Sulforaphane reduces hepatic glucose production and improves glucose control in patients with type 2 diabetes

Annika S. Axelsson,[1] Emily Tubbs,[1] Brig Mecham,[2] Shaji Chacko,[3] Hannah A. Nenonen,[1] Yunzhao Tang,[1] Jed W. Fahey,[4] Jonathan M. J. Derry,[5] Claes B. Wollheim,[1,6] Nils Wierup,[1] Morey W. Haymond,[3] Stephen H. Friend,[5] Hindrik Mulder,[1] Anders H. Rosengren[1,5,7]*

A potentially useful approach for drug discovery is to connect gene expression profiles of disease-affected tissues ("disease signatures") to drug signatures, but it remains to be shown whether it can be used to identify clinically relevant treatment options. We analyzed coexpression networks and genetic data to identify a disease signature for type 2 diabetes in liver tissue. By interrogating a library of 3800 drug signatures, we identified sulforaphane as a compound that may reverse the disease signature. Sulforaphane suppressed glucose production from hepatic cells by nuclear translocation of nuclear factor erythroid 2–related factor 2 (NRF2) and decreased expression of key enzymes in gluconeogenesis. Moreover, sulforaphane reversed the disease signature in the livers from diabetic animals and attenuated exaggerated glucose production and glucose intolerance by a magnitude similar to that of metformin. Finally, sulforaphane, provided as concentrated broccoli sprout extract, reduced fasting blood glucose and glycated hemoglobin (HbA1c) in obese patients with dysregulated type 2 diabetes.

INTRODUCTION

A large number of genetic variants and tissue gene expression profiles ("disease signatures") have been associated with complex polygenic diseases over the last decade (*1*). However, these data have not been maximally used to identify new therapies. One potentially interesting approach is to use genetic and gene expression data to interrogate libraries of drug signatures (*2*). A drug signature denotes differentially expressed genes between untreated and treated samples and takes into account that most compounds have multiple gene effects on expression beyond the primary target.

A few previous studies have used gene set enrichment analysis to connect disease signatures with drug signatures and identified candidate drugs for cancer, neurological, and gastrointestinal disorders, as suggested by subsequent effect studies in cell lines and animal models (*3*–*6*). However, it remains to be shown whether such signature connections can be used to identify compounds with pathophysiological relevance for humans. The usefulness of this approach for drug discovery may have been hampered by the fact that expression signatures from disease-affected tissues largely represent secondary changes. Moreover, the rank order of a gene in a signature based on expression fold change does not necessarily reflect the pathophysiological importance of the gene.

To overcome these limitations, we generated disease signatures based on disease-relevant tissue networks and human genetic data. Network models have been proposed as a useful framework for studying complex data (*7*). We and others have shown that highly connected network genes ("hub genes") are more likely to be involved in disease processes (*8*, *9*). Here, we hypothesized that disease signatures reflecting the network topology and not merely expression fold change could be used to identify compounds that reverse aberrantly expressed key drivers of disease (overexpressed genes should be downregulated in the drug signature and vice versa). To test this strategy, we analyzed diabetes-associated gene networks in liver tissue. We aimed to identify compounds to treat exaggerated hepatic glucose production in patients with type 2 diabetes (T2D), which is a clinically severe problem (*10*). T2D is affecting a growing number of the population, with more than 300 million people worldwide afflicted by the disease and even more having prediabetes (*11*). Metformin is currently the first-line therapy and reduces hepatic glucose production via adenosine monophosphate (AMP) kinase-dependent and kinase-independent mechanisms (*12*–*14*). However, 15% of all T2D patients cannot take metformin because of reduced kidney glomerular filtration rate and hence increased risk of lactic acidosis (*15*). Moreover, up to 30% of patients treated with metformin develop nausea, bloating, abdominal pain, or diarrhea, and 5 to 10% of the patients are therefore unable to continue with metformin (*16*). Finding additional treatment options to reduce exaggerated hepatic glucose production is therefore a high priority.

RESULTS

Network-based disease signatures were connected to drug signatures

We first analyzed global gene expression data in liver tissue from an F2 cross between C57BL/6J *ApoE*$^{-/-}$ and C3H/HeJ *ApoE*$^{-/-}$ mice with a total of 334 mice (169 female and 165 male). This cross, termed the B × H cross, recapitulates a range of phenotypes associated with the metabolic syndrome, including dyslipidemia, increased body weight, and hyperglycemia (*17*, *18*). We analyzed the topological overlap of the gene expression data and identified groups of coexpressed genes ("modules"), comprising a total of 1720 genes, which were associated with hyperglycemia.

[1]Department of Clinical Sciences, Lund University Diabetes Center, Malmö, SE-20502 Malmö, Sweden. [2]Trialomics, Seattle, WA 98115, USA. [3]U.S. Department of Agriculture/Agricultural Research Service, Children's Nutrition Research Center, Department of Pediatrics, Baylor College of Medicine, Houston, TX 77030, USA. [4]Departments of Medicine, Pharmacology and Molecular Sciences, and International Health, and Cullman Chemoprotection Center, Johns Hopkins University, Baltimore, MD 21205, USA. [5]Sage Bionetworks, 1100 Fairview Avenue North, Seattle, WA 98109, USA. [6]Department of Cell Physiology and Metabolism, University Medical Center, CH-1211 Geneva, Switzerland. [7]Institute of Neuroscience and Physiology, University of Gothenburg, SE-40530 Göteborg, Sweden.
*Corresponding author. Email: anders.rosengren@gu.se

We then used four different criteria to select those of the 1720 genes that were most likely to be involved in diabetes pathophysiology. First, we analyzed connectivity (k_{in}) as a measure of gene coexpression to identify highly connected network hubs (*7*). Second, we used Bayesian modeling to identify key regulators of the coexpression networks (*19*). Third, we used genetic risk variants associated with T2D to inform the generation of the disease signature by constructing a protein-protein interaction network with a total of 319 genes centered on those that are in close proximity of known T2D risk variants (*20*). Fourth, we used data on single-nucleotide polymorphisms associated with gene expression traits (eSNPs) in human liver samples to identify genes with eSNPs that were also risk variants for T2D, because such genes have been suggested to cause metabolic disease (*21*). The rationale for using these four criteria was to incorporate both network topology and genetic information to focus on those of the 1720 genes that were likely to have the highest pathophysiological impact based on previous reports on features that are important for metabolic disease networks (*8*, *17*, *19*, *21*).

A leave-one-out approach with linear modeling was used to impute weights for each criterion. The linear modeling was iterated for each of the four criteria variables. Solving the resultant equation system provided a coefficient for each variable, which was used as a weight to reflect the relative importance of the variable. Finally, we computed a score for each of the 1720 genes based on the four criteria and used it as a filter to generate a 50-gene disease signature for T2D in liver tissue (table S1).

We then compiled a library of 3852 drug signatures from publically available data sets at the Gene Expression Omnibus (GEO) or the European Bioinformatics Institute based on experiments with compound treatments of cell lines or primary tissues and analyzed by Affymetrix, Agilent, or Illumina chips (see table S2 for a list of the compounds). The hepatic diabetes signature and each of the drug signatures were analyzed using an enrichment metric based on a Kolmogorov-Smirnov (KS) test. The average KS enrichment metric for the 10 top-ranked drugs was significantly higher when using the filtered 50-gene disease signature compared with using 50 genes randomly selected out of the 1720 genes or using all 1720 genes (>2-fold higher KS scores; $P < 0.001$; the top-ranked drugs differed depending on which disease signature was used), suggesting that the disease signature filtered by the four criteria generates more robust data. The drug signature that exhibited the highest overlap with the 50-gene hepatic diabetes signature was derived from studies of sulforaphane (SFN)–treated human hepatocytes (GEO accession number GSE20479) (*22*). A complete rank list of all compounds is provided in table S3.

SFN reduces glucose production in hepatoma cells

Several other methods could potentially be used to compare disease and drug signatures, and it is critical that bioinformatics predictions are validated both in vitro and in vivo. We therefore investigated the compound with the highest overlap, SFN, in greater detail. SFN is a naturally occurring isothiocyanate found in cruciferous vegetables such as broccoli. It activates nuclear factor erythroid 2–related factor 2 (NRF2) by modifying the conformation of Kelch-like ECH-associated protein 1 (KEAP1) cytoplasmic chaperone, thus releasing NRF2 for translocation to the nucleus and transcriptional activation of genes with the antioxidant response element (ARE) in their promoters (*23*). Although SFN uptake into cells leads to an initial burst of reactive oxygen species, it then rapidly activates the KEAP1-NRF2-ARE system to induce antioxidant enzymes and increase cellular glutathione for an overall antioxidative effect (*24*). As an inducer of endogenous antioxidants, SFN has been extensively studied for its protective effects in different experimental models associated with oxidative stress and chemoprotection (*25*), inflammatory disorders (*26*), and fatty liver disease (*27*, *28*). To date, SFN has not been implicated for the treatment of exaggerated hepatic glucose production in T2D.

We first studied the effect of SFN on glucose production using H4IIE cells, a rat hepatoma cell line. Preincubation with SFN at 0.5 to 10 μM for 24 hours resulted in a dose-dependent decrease of glucose production during a subsequent 5-hour incubation in glucose-free buffer supplemented with gluconeogenetic substrates (41% decrease at 3 μM; $P = 0.0009$; Fig. 1A). SFN at doses up to 3 μM did not induce apoptosis (fig. S1A). Metformin also decreased glucose production in a dose-dependent manner (Fig. 1B). Addition of insulin to the buffer reduced glucose production by 40% in control cells. The combined effects of SFN and insulin on glucose production were only additive (Fig. 1A). In contrast, we observed synergistic effects of metformin and insulin on glucose production ($P = 0.005$ for analysis of additive versus synergistic effects at 250 μM metformin; Fig. 1B and Materials and Methods).

We also pretreated H4IIE cells with high concentrations of palmitate (250 μM) to mimic diabetogenic conditions. Palmitate pretreatment increased glucose production by 34%, in line with previous observations (*29*, *30*). Concomitant treatment with SFN not only prevented the exaggerated glucose production but also reduced overall glucose production by 45% ($P = 0.0011$; Fig. 1C).

The effect of SFN on glucose production is mediated by the transcription factor NRF2

We then investigated the effect of SFN on nuclear translocation of NRF2, which has been demonstrated as a major mechanism of action for SFN in other cell types (*31*). We observed a clear dose-dependent effect of SFN on nuclear translocation of NRF2 in the H4IIE cells (Fig. 1D). Silencing of *Nrf2* by small interfering RNA (siRNA) (81 ± 3% knockdown) increased glucose production 2.3-fold ($P = 0.0009$) and attenuated the relative effect of SFN on glucose production ($P = 0.007$; Fig. 1E). This suggests that a large part of SFN-mediated reduction of glucose production is mediated via NRF2, although we do not exclude that other mechanisms may also be involved.

SFN has no effect on insulin signaling and mitochondrial oxygen consumption

Because insulin is a key regulator of hepatic glucose production in the fed state, we next examined the effect of SFN on key enzymes in the insulin signaling cascade. However, in H411E cells, insulin-mediated phosphorylation of insulin receptor substrate 1 (IRS1/Tyr^{608}) and AKT serine/threonine kinase 1 (AKT1/Ser^{473}) was unaffected by SFN. Moreover, we observed no effect of SFN on insulin signaling after palmitate pretreatment (fig. S1B). The observations are in agreement with the data on glucose production (Fig. 1A), which suggest that the combined effects of SFN and insulin on glucose production are nonsynergistic and merely additive. These results show that the effect of SFN on glucose production is not mainly exerted via altered insulin signaling.

Because NRF2 affects the activity of complex 1 in the mitochondrial respiratory chain via limitation of substrates (*32*), we also investigated whether SFN affected mitochondrial function using the Seahorse XF24 instrument to measure the mitochondrial oxygen consumption rate (OCR) in H4IIE cells in response to gluconeogenetic substrates (L-lactate, pyruvate, and L-glutamine). However, SFN (3 μM) did not affect mitochondrial OCR under these experimental conditions (fig. S1C).

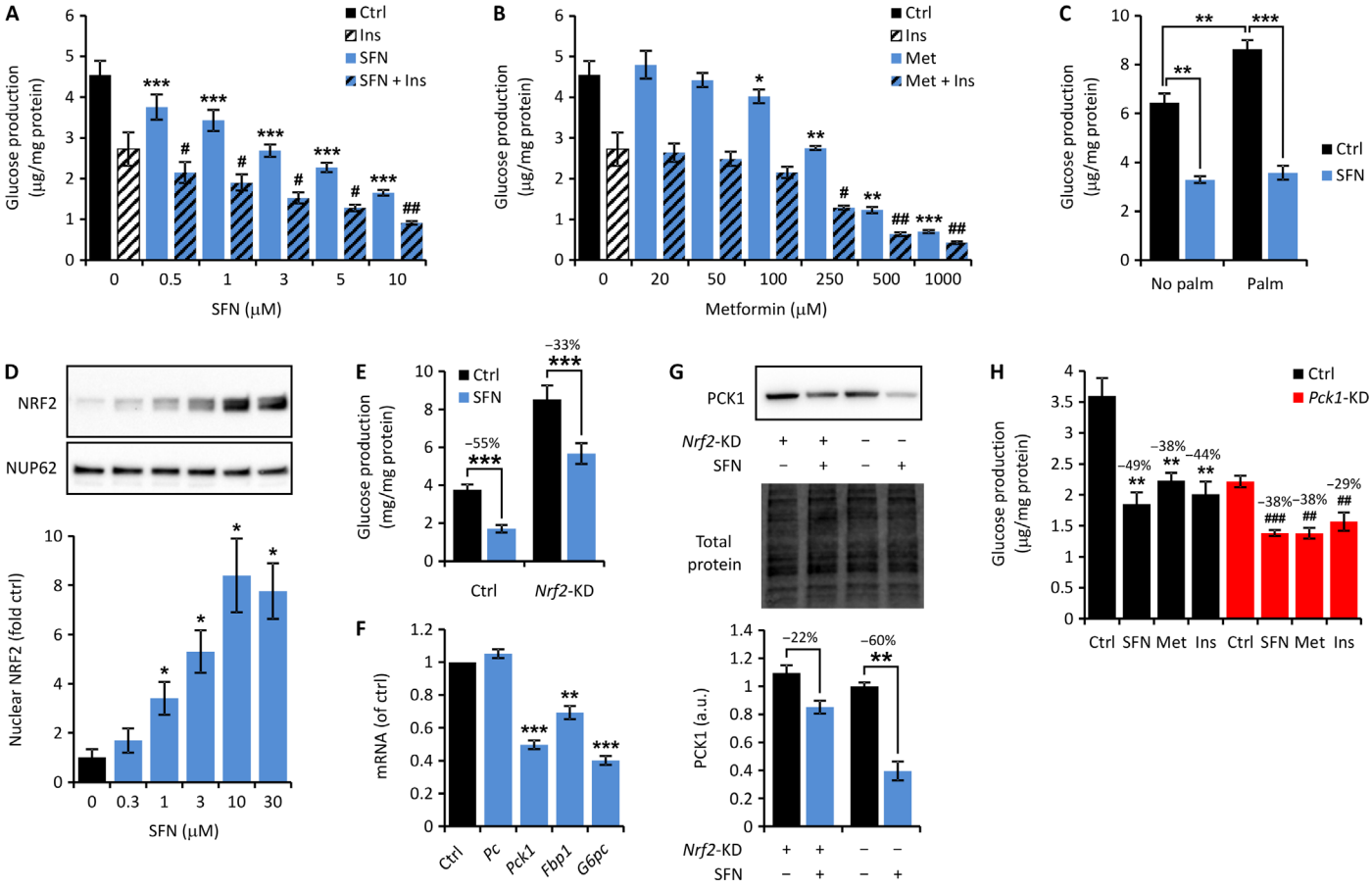

Fig. 1. Effects of SFN on glucose production in H4IIE hepatoma cells. Glucose production (GP) was assessed during a 5-hour incubation in glucose-free buffer with pyruvate, L-lactate, and L-glutamine (GP-buffer). (**A**) GP in the presence or absence of 10 nM insulin (INS) in the GP-buffer assessed after 24-hour preincubation with or without SFN as indicated ($n = 5$). * denotes control (ctrl) cells versus SFN-treated cells; # denotes insulin-treated cells in the absence versus presence of SFN. (**B**) As in (A), with or without metformin (met) preincubation for 24 hours instead of SFN ($n = 5$). (**C**) GP assessed after 16 hours of pretreatment with 250 μM palmitate (palm) followed by 24 hours with or without 3 μM SFN ($n = 4$). (**D**) Representative immunoblot and summary statistics showing nuclear translocation of NRF2 protein after 1 hour of incubation with SFN at the doses indicated. Nucleoporin 62 (NUP62) was used as loading control ($n = 3$). (**E**) GP after knockdown of *Nrf2* (*Nrf2*-KD) or treatment with a negative control siRNA followed by 24-hour preincubation with or without 3 μM SFN ($n = 5$). (**F**) mRNA expression of genes involved in gluconeogenesis after treatment with 3 μM SFN for 24 hours. Statistical analysis was performed using $\log_2$-transformed data ($n = 4$ to 6). (**G**) Representative immunoblot and summary statistics of PCK1 protein expression after knockdown of *Nrf2* (*Nrf2*-KD) or treatment with a negative control siRNA followed by 24-hour preincubation with or without 3 μM SFN ($n = 4$). a.u., arbitrary units. (**H**) GP after knockdown of *Pck1* (*Pck1*-KD) or treatment with a negative control siRNA. Cells were then treated with or without 3 μM SFN or 250 μM metformin for 24 hours as indicated ($n = 5$). * denotes control versus SFN, metformin, or insulin in cells treated with a negative control siRNA; # denotes control versus SFN, metformin, or insulin in *Pck1*-KD cells. Data are means ± SEM. $^{*}P < 0.05$; $^{**}P < 0.01$; $^{***}P < 0.001$; $^{\#}P < 0.05$; $^{\#\#}P < 0.01$.

SFN reduces the expression of genes involved in glucose production

To further explore the mechanism by which SFN affects glucose production, we analyzed the expression of genes involved in gluconeogenesis, a major determinant of hepatic glucose production. Of the four key enzymes involved in gluconeogenesis—pyruvate carboxylase (PC; $P = 0.2$), phosphoenolpyruvate carboxykinase 1 (PCK1; also known as PEPCK-C; $P = 0.004$), fructose-1,6-bisphosphatase 1 (FBP1; $P = 0.0007$), and glucose-6-phosphatase, catalytic subunit (G6PC; $P = 0.002$)—all except PC were significantly down-regulated by SFN, as assessed by expression microarrays of H4IIE cells (table S4). Quantitative reverse transcription polymerase chain reaction of H4IIE cells treated with 3 μM SFN for 24 hours confirmed these findings, with *Pck1* and *G6pc* being the gluconeogenesis genes most strongly down-regulated by SFN (Fig. 1F). PCK1 is of special interest because it catalyzes the conversion of oxaloacetate to phosphoenolpyruvate, the rate-limiting step in gluconeogenesis. SFN reduced PCK1 protein by 60% in H4IIE cells ($P = 0.0011$; Fig. 1G). We also analyzed the effects of SFN on PCK1 protein after *Nrf2* knockdown and observed a mere 22% reduction of PCK1, which is a significant attenuation compared with the 60% reduction in control cells ($P = 0.0082$ for the comparison of SFN effects in *Nrf2*-KD versus control cells; Fig. 1G). This suggests that PCK1 down-regulation by SFN is largely mediated via NRF2.

We next silenced *Pck1* with siRNA (*Pck1*-KD) in H4IIE cells (69 ± 2% knockdown), which resulted in a 38% reduction of glucose production. The inhibitory effect of SFN on glucose production was attenuated by 23% (49% reduction of glucose production by SFN in control cells compared to 38% reduction in *Pck1*-KD cells; $P = 0.025$; Fig. 1H). In contrast, the effect of metformin (250 μM) was unaffected by *Pck1*-KD (38% reduction in both cases), showing that metformin-induced

suppression of glucose production is independent of PCK1. We also observed that the effect of insulin was significantly reduced (33% reduction of effect size; $P = 0.037$) in *Pck1*-KD cells, confirming previous observations that PCK1 is regulated by insulin (*33*). Together, these data suggest that a major mechanism for SFN-mediated reduction of glucose production is down-regulation of key gluconeogenetic enzymes via NRF2. The mechanism of action of SFN is therefore different from that of metformin, which acts via AMP-activated protein kinase, by lowering cyclic AMP and inhibiting mitochondrial glycerophosphate dehydrogenase (*12*–*14*). As with metformin, which has multiple modes of action, we do not exclude that additional mechanisms may contribute to the effects of SFN on glucose production.

SFN reduces glucose production in mouse hepatocytes

We also verified that SFN affects glucose production in primary mouse hepatocytes. Hepatocytes were incubated with SFN in the presence of palmitate for 24 hours before the experiments to mimic a diabetogenic milieu. Palmitate incubation increased glucose production 2.2-fold. SFN induced a 45% reduction of glucose production in palmitate-exposed hepatocytes ($P = 0.042$; Fig. 2A) and restored glucose production to levels observed in the absence of palmitate. These data corroborate the observations in H4IIE cells and show that SFN treatment suppresses exaggerated glucose production triggered by a diabetogenic milieu in vitro.

SFN prevents the development of glucose intolerance in diet-challenged rats

After these experiments, we aimed to investigate the effect of SFN in different animal models in vivo. We first assessed the ability of SFN to prevent the development of glucose intolerance. Male Wistar rats received a diet with 45% fat content [high-fat diet (HFD)] and were concomitantly treated with SFN [2.5 mg/kg, intraperitoneally (ip), three times per week] or vehicle over 15 weeks. In vehicle-treated animals, fasting blood glucose, which reflects hepatic glucose production, increased by 16% during the 15-week period on HFD ($P = 0.0014$). By contrast, there was no impairment of fasting glucose in SFN-treated rats (Fig. 2B). Over the entire period, fasting blood glucose was significantly lower in SFN-treated compared to nontreated rats (on average 7.5% lower; $P = 2 \times 10^{-5}$; Fig. 2B). At the end of the 15-week period, there was also a significant difference in insulin sensitivity between the SFN-treated group and the nontreated group as measured by an intraperitoneal insulin tolerance test (IPITT) [$P = 0.032$ for area under the curve (AUC); Fig. 2C].

To further explore the ability of SFN to prevent glucose intolerance under different dietary conditions, we changed diets after 15 weeks on 45% HFD. Half of the rats received instead a diet with even higher fat content (60%), and half received a diet with 60% fructose content [high-fructose diet (HFrD)] with continued treatment with SFN or vehicle. SFN improved glucose tolerance, assessed by an intraperitoneal glucose tolerance test (IPGTT) after 5 weeks on 60% HFrD ($AUC_{30–120}$ $P = 0.025$, Fig. 2D; Fig. 2E for IPITT). In rats on 60% HFD, SFN did not affect glucose tolerance (Fig. 2F) but changed insulin sensitivity as assessed by an IPITT (AUC $P = 0.0038$; Fig. 2G). These findings show that SFN was able to prevent the development of diet-induced glucose intolerance induced by a 45% HFD or a 60% HFrD, although the 60% HFD was too severe a stressor to fully prevent glucose intolerance by SFN.

We also extracted liver tissue from rats on 60% HFrD treated with SFN (2.5 mg/kg) three times a week for 27 weeks and analyzed global gene expression by microarray. We analyzed the effect of SFN on the 50-gene hepatic disease signature and observed that a significant fraction of the signature was reversed in SFN-treated rats compared with vehicle-treated animals ($P < 0.0001$, Fisher's exact test; fig. S2).

SFN improves glucose tolerance in rats on HFD or HFrD

On the basis of the observation that SFN prevents diet-induced glucose intolerance, we next wanted to test whether SFN could be used to treat rats that had already developed glucose intolerance. Male Wistar rats were therefore put on a 60% HFD for 11 months and then received SFN (5 mg/kg, ip) daily for 14 days. Treatment with SFN resulted in improved glucose tolerance, as assessed by an oral glucose tolerance test (OGTT) ($P = 0.049$ for $AUC_{30–120}$; Fig. 2H).

We next compared the effects of SFN and metformin on glucose tolerance and hepatic glucose production in vivo. Male Wistar rats that had been fed a 60% HFrD for 6 months were treated with either SFN (10 mg/kg, ip) or metformin [300 mg/kg, per os (po)] for 9 to 12 days. Glucose tolerance was significantly improved by both SFN and metformin during an OGTT ($AUC_{30–120}$ $P = 0.046$ for SFN-treated versus untreated rats and $P = 0.019$ for metformin-treated versus untreated rats; Fig. 2I). On the basis of our observations in H4IIE cells and primary hepatocytes, we hypothesized that SFN would reduce hepatic glucose production. Hepatic glucose production was assessed by an intraperitoneal pyruvate tolerance test (IPPTT), which showed that SFN significantly reduced blood glucose at 30 and 120 min and reduced $AUC_{30–120}$ by 20% ($P = 0.049$, one-sided *t* test; Fig. 2J). Metformin significantly reduced blood glucose at 60 min during the IPPTT and reduced $AUC_{30–120}$ by 25% ($P = 0.046$, one-sided *t* test). These results demonstrate that SFN improves glucose tolerance in rats by a magnitude similar to that of metformin.

SFN improves glucose tolerance in mice with diet-induced diabetes

To test the effect of SFN in a more severe model of diabetes, we used C57BL/6J mice, which develop overt diabetes when challenged with an HFD. After 10 weeks on a 60% HFD, male C57BL/6J mice were treated with SFN (10 mg/kg) daily for 4 weeks (same dose as used in the rat experiments). We also tested the effect of a considerably lower dose (0.5 mg/kg SFN daily). The high dose of SFN improved both fasting glucose ($P = 0.044$) and glucose tolerance ($AUC_{30–120}$ $P = 0.012$; Fig. 3A) as measured by an IPGTT. In this model, SFN did not affect insulin sensitivity (Fig. 3B). The low dose of SFN had no effect on glucose tolerance. Extracted liver from the mice treated with SFN at high dose had reduced triglyceride content relative to mice receiving the low dose ($P = 0.038$; Fig. 3C). In lean mice receiving a low-fat control diet, glucose tolerance was unaffected by SFN (Fig. 3A).

We next performed specific measurements of absolute gluconeogenetic rate in C57BL/6J mice on 60% HFD using mass spectrometry of glucose fragments after ingestion of deuterium water combined with hyperinsulinemic-euglycemic clamps. The mice were treated with SFN (10 mg/kg) or control vehicle daily for 4 weeks. After a 7- to 9-hour fast and a 2-hour infusion of [6,6-$^2H_2$]glucose, glucose production was almost entirely derived from gluconeogenesis (101 ± 2% for control and 97 ± 3% for SFN-treated mice). In the controls, we observed a clear correlation between body weight of the mice (range, 36 to 47 g) and gluconeogenetic rate ($R^2 = 0.81$; $P = 0.002$). This is in line with reports in humans showing that glucose production is exaggerated in obese compared to lean subjects (*34*–*36*). In SFN-treated mice, the correlation between weight and increased gluconeogenesis was completely abolished ($R^2 = 0.11$; $P = 0.5$), suggesting that SFN protects against increased gluconeogenesis in the overweight animals. There was no difference when

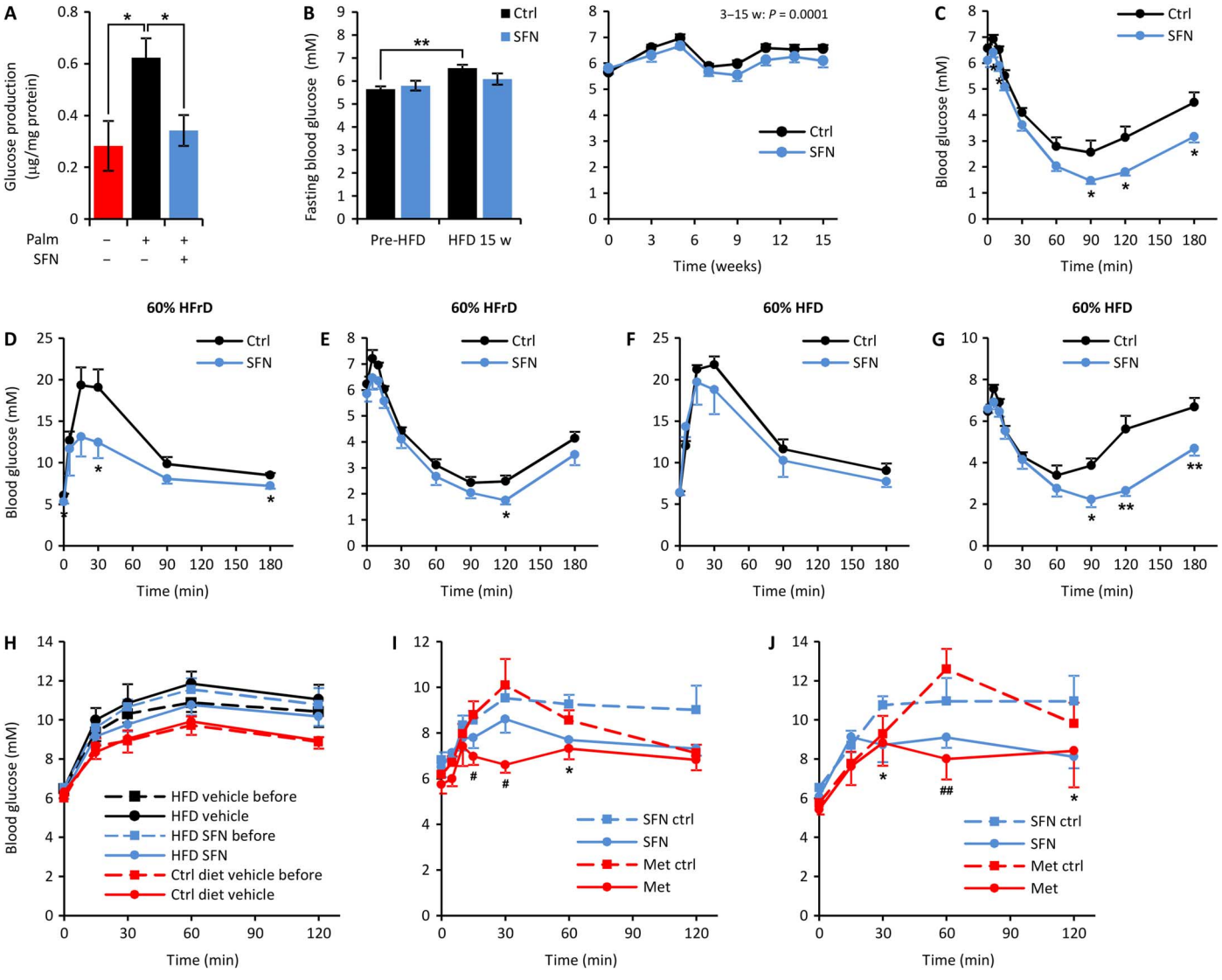

Fig. 2. Effects of SFN in mouse hepatocytes and in rat models of diet-induced glucose intolerance. (**A**) Glucose production from primary mouse hepatocytes during 45 min. Cells were preincubated in the presence or absence of 500 µM bovine serum albumin–bound palmitate followed by 24-hour incubation with or without 3 µM SFN as indicated ($n = 3$). (**B**) Left: Fasting blood glucose in male Wistar rats before and after 15 weeks of HFD feeding with or without concomitant SFN treatment [SFN (2.5 mg/kg) three times per week; $n = 9$ per group]. Right: Longitudinal measurements of fasting glucose during the 15-week period. *P* value for the blood glucose for the SFN-treated compared to control-treated rats during the 3- to 15-week period is shown. (**C**) IPITT after the 15-week period for the same rats as in (B). (**D** to **G**) Insulin resistance (IR) and glucose tolerance assessed in the same animals as in (B) after an additional 5 weeks on 60% HFrD or HFD with or without concomitant SFN treatment. IPGTT (D) and IPITT (E) data from rats on 60% HFrD ($n = 4$ to 5 per group), and IPGTT (F) and IPITT (G) data from rats on 60% HFD ($n = 4$ to 5 per group). (**H**) OGTT data from male Wistar rats fed a low-fat control diet (ctrl diet) or a 60% HFD for 11 months before and after 14 days of treatment with SFN (5 mg/kg per day) or vehicle ($n = 5$ HFD ctrl, $n = 6$ HFD SFN, and $n = 8$ ctrl diet). (**I**) OGTT in male Wistar rats with diet-induced glucose intolerance (fed 60% HFrD for 6 months) after 10 days of treatment with or without SFN (10 mg/kg per day, ip) or metformin (300 mg/kg, po) as indicated. * denotes SFN ($n = 6$) versus vehicle ($n = 7$); # denotes metformin ($n = 6$) versus the corresponding vehicle ($n = 8$). (**J**) IPPTT on the same rats as in (I) after 9 to 12 days of treatment with or without SFN or metformin as indicated. One-sided *t* test was used for statistical analysis. * denotes SFN ($n = 6$) versus vehicle ($n = 7$); # denotes metformin ($n = 6$) versus the corresponding vehicle ($n = 7$). Data are means ± SEM. $^{*}P < 0.05$; $^{**}P < 0.01$; $^{\#}P < 0.05$; $^{\#\#}P < 0.01$.

taking all animals into account, independent of weight. However, by using a post hoc analysis of the heaviest mice, we observed that SFN significantly reduced absolute gluconeogenesis rate compared to controls in this subset (6.5 mg/kg per minute in control and 5.6 mg/kg per minute in SFN-treated mice; $P = 0.035$; Fig. 3D).

During the clamp, we also measured total body insulin-stimulated glucose uptake (Rd clamp), which reflects insulin sensitivity. This was similar between the groups [ctrl (11.8 mg/kg) and SFN (12.8 mg/kg); Fig. 3E], which parallels our findings in H4IIE cells that SFN does not influence insulin signaling. Together, these experiments demonstrate that SFN improves glucose tolerance in animals with diet-induced diabetes via reduced gluconeogenetic rate.

The effect of SFN-containing broccoli sprout extracts was studied in T2D patients

Prompted by these findings in vitro and in vivo, we set out to investigate the effects of SFN on glucose control in T2D patients. SFN has been provided at high concentration as broccoli sprout extracts (BSEs) in

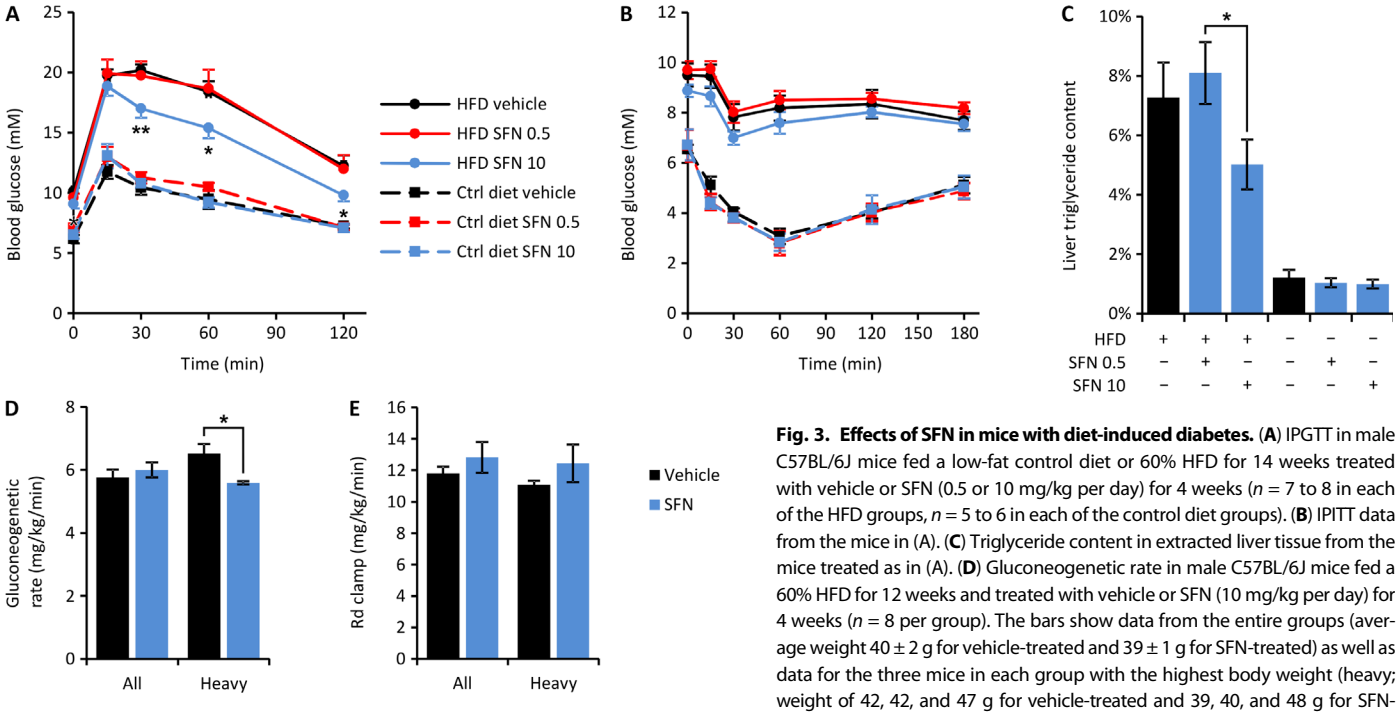

Fig. 3. Effects of SFN in mice with diet-induced diabetes. (**A**) IPGTT in male C57BL/6J mice fed a low-fat control diet or 60% HFD for 14 weeks treated with vehicle or SFN (0.5 or 10 mg/kg per day) for 4 weeks ($n = 7$ to 8 in each of the HFD groups, $n = 5$ to 6 in each of the control diet groups). (**B**) IPITT data from the mice in (A). (**C**) Triglyceride content in extracted liver tissue from the mice treated as in (A). (**D**) Gluconeogenetic rate in male C57BL/6J mice fed a 60% HFD for 12 weeks and treated with vehicle or SFN (10 mg/kg per day) for 4 weeks ($n = 8$ per group). The bars show data from the entire groups (average weight 40 ± 2 g for vehicle-treated and 39 ± 1 g for SFN-treated) as well as data for the three mice in each group with the highest body weight (heavy; weight of 42, 42, and 47 g for vehicle-treated and 39, 40, and 48 g for SFN-treated compared to an average weight of 38 ± 1 g for vehicle-treated and 37 ± 0.2 g for SFN-treated nonheavy mice). (**E**) Rate of disappearance of glucose (Rd) during clamp, reflecting whole-body insulin-stimulated glucose uptake, for the same mice as in (D). Data are means ± SEM. *$P < 0.05$; **$P < 0.01$.

several clinical studies for cancer, chronic obstructive pulmonary disease, autism, and inflammatory diseases (www.clinicaltrials.gov) [we used high-performance liquid chromatography (HPLC)–purified SFN at 99.5% in our cell and animal studies, but this has not been used for human studies so far].

Here, we used a dried powder of an aqueous extract of broccoli sprouts, which contains high concentrations of glucoraphanin, the inert glucosinolate precursor of SFN. Glucoraphanin is converted to SFN by the release of intrinsic sprout myrosinase during chewing and also by human enteric bacteria (*37*–*40*). After intake, the plasma concentration of SFN rises within 1 hour with a mean half-life of 1.77 ± 0.13 hours, but SFN exerts a sustained effect on gene expression (*41*). Renal tubular secretion is suggested to play a major role in the elimination (*37*). Safety studies using BSE corresponding to 50 to 400 μmol SFN daily have shown that BSE is well tolerated without clinically significant adverse effects (*42*–*45*).

We first tested the effect of BSE relative to HPLC-purified SFN on hepatic glucose production in H4IIE cells. The amount of SFN in BSE (SFN equivalents) was determined on the basis of the concentration of SFN obtained when glucoraphanin in BSE is hydrolyzed by adding exogenous myrosinase. We confirmed that BSE (at 3 μM SFN equivalents) was as effective as HPLC-purified SFN (3 μM) in suppressing glucose production ($P = 0.004$ for BSE and $P = 0.004$ for SFN relative to control; fig. S3A). No exogenous myrosinase was added during the experiment, demonstrating that the BSE contained sufficient amounts of myrosinase to effectively convert inert glucoraphanin to SFN.

Next, we wanted to ascertain that the effect of BSE on glucose production was caused by the SFN component. We therefore boiled the BSE, which inactivates myrosinase and prevents the conversion of glucoraphanin to SFN (*46*). After boiling, BSE had no effect on glucose production (fig. S3A). We also showed that the placebo (maltodextrin sprayed with copper-chlorophyllin) to be used in the clinical trial had no effect on glucose production. Moreover, we verified that BSE had a similar effect to that of SFN on glucose control in animals. Male C57BL/6J mice were made diabetic by a 60% HFD for 4 weeks and were then given BSE via gavage once daily at a dose corresponding to SFN (1.1 mg/kg) for 4 weeks. The BSE-treated mice had significantly lower fasting blood glucose compared to controls (9.6 versus 10.9 mM; $P = 0.009$) and improved glucose control during an IPGTT (fig. S3B).

After these verifications, we recruited 103 T2D patients for a randomized double-blind placebo-controlled study with BSE for 12 weeks. Patients with either well-regulated or dysregulated T2D (defined as having HbA1c above 50 mmol/mol) were recruited. All patients were of Scandinavian ethnicity and had been diagnosed with T2D less than 10 years ago. We hypothesized that BSE would improve fasting glucose (reflecting hepatic glucose production) and reduce HbA1c in patients with dysregulated T2D but have no effect in patients with well-regulated T2D, because well-regulated T2D patients exhibit impaired peripheral glucose uptake rather than exaggerated glucose production (*47*). The patients with dysregulated T2D were further divided into nonobese and obese [body mass index (BMI) > 30 kg/m^2], because hepatic glucose production has been shown to be more severely affected in obese compared to lean patients (*34*–*36*).

A total of 97 patients completed the study, of whom 60 had well-regulated and 37 dysregulated T2D. Of the patients with dysregulated T2D, 20 were nonobese and 17 were obese. All patients except three (well-regulated) had metformin treatment. The patients underwent initial blood sampling, including fasting glucose and HbA1c, and an OGTT, after which they received oral BSE or placebo once daily for 12 weeks. The BSE contained 150 μmol SFN per dose, which corresponds to one-third of the dose per body surface area compared with the animal experiments (using 10 mg/kg). This dose has been well

tolerated in clinical safety studies (*42*–*45*). A second OGTT and blood sampling were conducted at the end of the 12-week treatment period. The difference in fasting blood glucose (Δglucose) and HbA1c (ΔHbA1c) before and after treatment were determined for each patient.

BSEs improves fasting glucose and HbA1c in obese patients with dysregulated T2D

We observed a clear association between HbA1c levels at start of treatment and ΔHbA1c in response to BSE treatment (ΔHbA1c, 0.2 mmol/mol reduction per 1 mmol/mol higher HbA1c at start; $P = 0.004$, Fig. 4A), whereas there was no association in the placebo group ($P = 0.5$). There was also an association between BMI and ΔHbA1c in BSE-treated patients (ΔHbA1c, 0.4 mmol/mol reduction per 1 kg/m^2 higher BMI; $P = 0.015$ for the BSE group; not significant for the placebo group).

We then analyzed the patients with dysregulated T2D in detail, using intraindividual one-tailed comparisons before and after treatment. There was a significant change of fasting blood glucose (Δglucose) in BSE-treated compared with placebo-treated subjects ($P = 0.023$). Fasting plasma glucose was on average 9 ± 0.4 mM after placebo treatment and 8.3 ± 0.3 mM after BSE treatment. There was, however, no difference in ΔHbA1c between BSE and placebo in the entire group of patients with dysregulated T2D. In obese patients (BMI > 30 kg/m^2) with dysregulated T2D, who we hypothesized would benefit most from the treatment, both Δglucose ($P = 0.036$) and ΔHbA1c ($P = 0.034$) were significantly affected by BSE (Fig. 4B and Table 1). At the end of the 12-week period, HbA1c was 57 mmol/mol in placebo-treated and 53 mmol/mol in BSE-treated patients (ΔHbA1c, −4 mmol/mol; $P = 0.034$). There was a concomitant decrease of fasting blood glucose (8.9 mM with placebo and 8.2 mM with BSE; $P = 0.036$ for Δglucose; Fig. 4B) in these patients.

We also analyzed the serum concentration of SFN at the final visit (immediately before the OGTT) in the obese patients with dysregulated T2D using HPLC. SFN serum concentration ranged from 0.6 to 1.8 nmol/ml in BSE-treated patients (the concentration was 0.01 nmol/ml in placebo-treated subjects). The variation may be attributed to individual differences in bioavailability, body weight, and distribution volume. There was a clear association between serum SFN concentration and change in fasting blood glucose (Δglucose) in the BSE-treated patients ($P = 0.002$, corrected for body weight; Fig. 4C). The serum concentrations of SFN in BSE-treated patients (0.6 to 1.8 μM) were in the same range as the concentrations that reduced glucose production in vitro in H4IIE cells (Fig. 1A).

Previous studies using ^{13}C magnetic resonance spectroscopy have demonstrated that elevated fasting glucose production in T2D patients could be entirely attributed to increased gluconeogenesis. Our data from H4IIE cells show that SFN affects glucose production by reducing the expression of genes involved in gluconeogenesis rather than affecting insulin sensitivity. Moreover, SFN reduced gluconeogenetic rate in

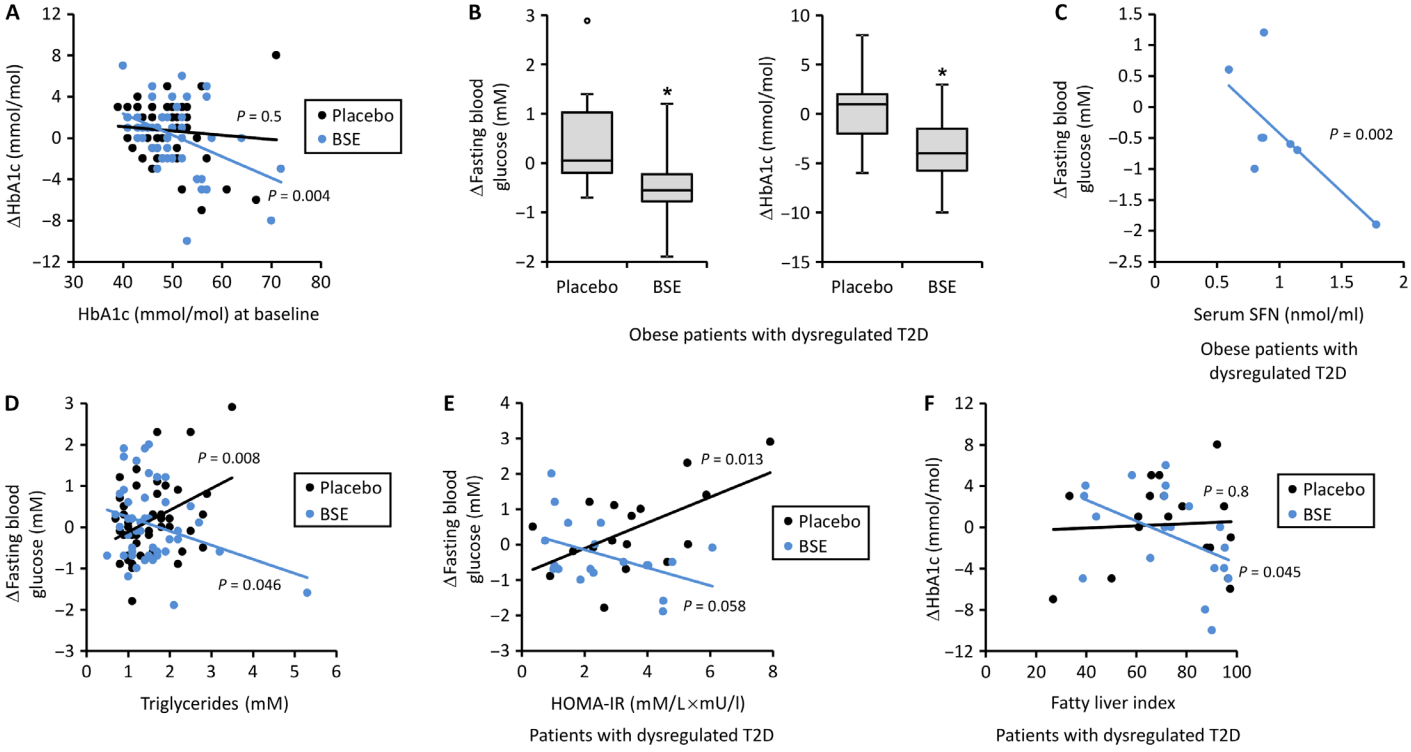

Fig. 4. Effects of highly concentrated SFN provided as BSE in T2D patients. (**A**) Association between HbA1c at the start of the study (baseline) and treatment-induced change in HbA1c (ΔHbA1c) after 12 weeks in all patients ($n = 50$ placebo and $n = 47$ BSE). (**B**) Box plots showing median, upper and lower quartiles, and maximum and minimum values of treatment-induced change in fasting blood glucose and HbA1c in obese patients with dysregulated T2D ($n = 9$ placebo and $n = 8$ BSE). Circle denotes outlier. (**C**) Association between serum concentration of SFN (after 12 weeks of treatment) and treatment-induced change in fasting blood glucose in obese patients with dysregulated T2D ($n = 8$ BSE). (**D**) Association between treatment-induced change in fasting blood glucose and plasma triglyceride concentrations at the start of the study in all patients ($n = 50$ placebo and $n = 47$ BSE). (**E**) Association between treatment-induced change in fasting blood glucose and HOMA-IR at the start of the study in patients with dysregulated T2D ($n = 18$ placebo and $n = 19$ BSE). (**F**) Association between treatment-induced change in HbA1c and fatty liver index at the start of the study in patients with dysregulated T2D ($n = 18$ placebo and $n = 19$ BSE). *$P < 0.05$.

Table 1. Effects of 12 weeks of treatment with BSE on clinical variables in T2D patients. Data are means ± SD for patients with well-regulated (HbA1c ≤ 50 mmol/mol) and with dysregulated T2D (HbA1c > 50 mmol/mol) who are nonobese (BMI ≤ 30 kg/m^2) or obese (BMI > 30 kg/m^2). Data measured before treatment start (baseline) and after 12 weeks on placebo or BSE.

Treatment	Phenotype	Time	Well-regulated T2D		Dysregulated T2D	
			Nonobese (*n* = 28)	Obese (*n* = 31)	Nonobese (*n* = 21)	Obese (*n* = 17)
Placebo	HbA1c (mmol/mol)	Baseline	46.4 ± 2.8	45.6 ± 3.4	54.6 ± 3.2	56.3 ± 7.5
		12 weeks	47.5 ± 4.1	46.3 ± 3.4	54.9 ± 4.4	56.6 ± 9.2
	Fasting P-glucose (mM)	Baseline	7.51 ± 0.91	7.26 ± 0.86	8.84 ± 0.84	8.33 ± 1.03
		12 weeks	7.55 ± 0.84	7.29 ± 0.87	9.08 ± 1.31	8.91 ± 1.75
	P-glucose 120 min (mM)	Baseline	13.77 ± 3.16	11.55 ± 2.58	17.00 ± 3.14	15.81 ± 2.50
		12 weeks	13.27 ± 3.58	11.22 ± 2.02	17.10 ± 3.82	15.28 ± 3.42
	BMI (kg/m^2)	Baseline	27.6 ± 1.9	33.3 ± 2.4	28.0 ± 1.3	33.1 ± 2.0
		12 weeks	27.8 ± 1.9	33.4 ± 2.5	28.1 ± 1.5	33.0 ± 2.1
	HOMA-IR (mM × mU/liter)	Baseline	1.75 ± 0.78	2.73 ± 1.50	2.36 ± 1.52	4.32 ± 1.80
		12 weeks	1.83 ± 0.86	3.04 ± 2.10	2.52 ± 1.70	5.11 ± 3.30
	ISI	Baseline	3.39 ± 1.59	2.47 ± 1.90	3.48 ± 2.69	1.60 ± 0.73
		12 weeks	3.70 ± 2.04	2.55 ± 2.08	3.41 ± 2.39	1.67 ± 0.79
	Fatty liver index	Baseline	60.2 ± 18.1	83.1 ± 13.9	58.0 ± 18.7	87.9 ± 10.8
		12 weeks	58.0 ± 17.7	81.2 ± 16.6	57.5 ± 22.2	87.9 ± 10.9
	P-triglycerides (mM)	Baseline	1.49 ± 0.65	1.39 ± 0.56	1.50 ± 0.49	1.88 ± 0.89
		12 weeks	1.40 ± 0.67	1.26 ± 0.42	1.40 ± 0.55	1.94 ± 0.89
BSE	HbA1c (mmol/mol)	Baseline	45.7 ± 3.2	46.1 ± 3.0	55.7 ± 6.0	57.1 ± 6.6
		12 weeks	46.9 ± 3.5	46.7 ± 2.7	57.3 ± 5.2	53.4 ± 6.8
	Fasting P-glucose (mM)	Baseline	7.49 ± 1.16	7.34 ± 0.94	8.61 ± 1.41	8.58 ± 1.60
		12 weeks	7.91 ± 1.68	7.60 ± 1.36	8.39 ± 1.24	8.15 ± 1.26
	P-glucose 120 min (mM)	Baseline	13.99 ± 4.22	13.33 ± 3.84	15.52 ± 3.26	15.64 ± 3.63
		12 weeks	13.83 ± 4.27	13.36 ± 3.17	16.51 ± 3.09	15.41 ± 3.61
	BMI (kg/m^2)	Baseline	28.1 ± 1.4	32.9 ± 1.8	27.8 ± 1.3	33.2 ± 2.1
		12 weeks	28.2 ± 1.4	33.4 ± 2.3	27.7 ± 1.3	33.1 ± 2.3
	HOMA-IR (mM × mU/liter)	Baseline	1.76 ± 0.76	2.46 ± 1.42	2.32 ± 1.77	3.02 ± 1.34
		12 weeks	2.44 ± 0.88	3.08 ± 1.50	2.20 ± 1.62	3.05 ± 0.87
	ISI	Baseline	2.78 ± 0.89	2.00 ± 0.84	4.08 ± 2.09	2.32 ± 1.03
		12 weeks	2.40 ± 1.00	1.92 ± 0.76	3.92 ± 1.98	2.28 ± 1.05
	Fatty liver index	Baseline	60.6 ± 18.7	83.2 ± 10.4	61.5 ± 18.8	87.7 ± 9.8
		12 weeks	62.9 ± 18.4	85.6 ± 10.3	62.4 ± 18.2	87.2 ± 7.6
	P-triglycerides (mM)	Baseline	1.42 ± 0.64	1.35 ± 0.40	1.87 ± 1.33	1.50 ± 0.53
		12 weeks	1.46 ± 0.65	1.42 ± 0.42	2.10 ± 1.23	1.40 ± 0.48

heavy C57BL/6J mice with diet-induced diabetes but had no effect on total body insulin-stimulated glucose uptake. The patient data are also compatible with a direct effect on the rate of gluconeogenesis, because BSE reduced fasting glucose and decreased HbA1c without any concomitant effect on hepatic IR, measured as homeostatic model assessment (HOMA)–IR, insulin sensitivity index (ISI), or glucose concentration at

2 hours of the OGTT (Table 1). There was a clear association between the reduction of fasting blood glucose (Δglucose) and the decrease in HbA1c (ΔHbA1c) in patients with dysregulated T2D ($P = 0.019$). This association was also significant after correction for HOMA-IR, ISI, and 2-hour glucose ($P = 0.0003$), suggesting that the change in HbA1c was mainly caused by reduced fasting blood glucose. We also estimated hepatic fat content using a validated fatty liver index (*48*) but observed no effect of BSE on this metric (Table 1). BSE did not change body weight, BMI, liver parameters, cholesterol concentration, plasma triglycerides, or blood hemoglobin concentration. BSE had no effect in patients with well-regulated T2D. It remains possible, however, that higher doses of SFN could also affect IR, in addition to the pronounced direct effect on the expression of gluconeogenesis genes.

BSE is most effective in obese patients with dysregulated T2D

Glucose production is exaggerated in dysregulated T2D, which is reflected in the higher fasting blood glucose among the patients with dysregulated T2D in our study (8.6 ± 0.2 in patients with dysregulated T2D versus 7.5 ± 0.2 mM in patients with well-regulated T2D; $P = 0.0001$). Consequently, BSE reduced fasting glucose in patients with dysregulated T2D but not in patients with well-regulated T2D ($P = 0.023$). We also observed an association between BMI and BSE-induced change in HbA1c ($P = 0.017$), and HbA1c was significantly reduced after BSE treatment in obese patients with dysregulated T2D ($P = 0.034$; Fig. 4B). BSE was more effective in lowering fasting blood glucose in patients with elevated plasma triglyceride concentrations ($P = 0.046$ for the association between plasma triglycerides at study start and Δglucose; an inverted association was observed in placebo-treated patients; $P = 0.008$; Fig. 4D). It is also notable that BSE was more effective in lowering fasting blood glucose in patients with high HOMA-IR ($P = 0.058$ for the association between HOMA-IR and Δglucose; Fig. 4E), and the BSE-induced reduction of HbA1c correlated with high fatty liver index ($P = 0.045$; Fig. 4F).

No severe adverse effects of BSE were reported

Most patients tolerated the BSE well. Eight patients receiving BSE and seven patients receiving placebo reported gastrointestinal side effects such as loose stools and flatulence, typically present during the first few days of the treatment period, after which these symptoms disappeared. Ten BSE-treated and five placebo-treated patients reported mild respiratory infections, and there were also a few other reported adverse events, including orthopedic ailments, most likely unrelated to the study compound (table S5). Of the 103 patients, 6 (5 with BSE and 1 with placebo) discontinued the study because of nausea (2 patients), headache (1 patient), glucose above 15 mM (one of the exclusion criteria; 1 patient), hospital visit for suspected ileus (later successfully treated; 1 patient), and depression (1 patient on placebo) (table S6).

DISCUSSION

Together, our data show that SFN reduces glucose production, partly via NRF2 translocation and decreased expression of key gluconeogenetic enzymes, and that highly concentrated SFN administered as BSE improves fasting glucose and HbA1c in obese patients with dysregulated T2D. BSE was well tolerated, and SFN reduced glucose production by mechanisms different from that of metformin. SFN also protects against diabetic complications such as neuropathy, renal failure, and atherosclerosis in animal models because of its antioxidative effects (*49*–*52*).

Our data suggest that BSE has a direct effect on gluconeogenesis rather than hepatic insulin sensitivity, but the degree of IR may still influence the efficacy of BSE via altered constitutive NRF2 activity. It has been shown that insulin signaling activates NRF2 via phosphatidylinositide 3-kinase (*53*). Moreover, studies in cardiomyocytes have shown that NRF2 is activated at the early stages of T2D to protect against increased reactive oxygen species but is reduced at later stages of the disease (*54*). This is further supported by observations of reduced NRF2 expression in animals with IR (*55*, *56*) and hepatic steatosis (*27*, *28*).

It is not surprising that BSE was most effective in obese patients with dysregulated T2D. First, our animal experiments showed an effect of SFN on glucose control in metabolically dysregulated animals on a HFD but not in metabolically well-regulated animals on a low-fat diet. Second, gluconeogenetic rate was correlated with body weight in mice with diet-induced diabetes, and SFN reduced gluconeogenetic rate specifically in the heaviest mice. Third, hepatic glucose production is often exaggerated in patients with high HbA1c, whereas patients with low HbA1c primarily have an impairment of peripheral glucose uptake (*47*). Fourth, it has been shown that hepatic glucose production is increased particularly in obese T2D patients, potentially via elevated free fatty acids (*34*–*36*).

There is abnormal regulation of hepatic glucose production early in the development of T2D, but it is typically compensated for by increased insulin secretion (*57*). SFN has been shown to protect from pancreatic β cell damage in animals (*58*). We observed no changes in insulin secretion, measured as HOMA-B and insulinogenic index, and BSE did not affect fasting glucose or HbA1c in well-regulated T2D patients. However, we observed that SFN prevented the development of hyperglycemia in diet-challenged rats, and it would be of interest to longitudinally study the long-term effects of BSE on glucose production and insulin secretion capacity in prediabetic individuals.

Glitazones and metformin were not ranked particularly high in the drug comparisons, suggesting that they do not affect the hepatic gene coexpression network that was associated with hyperglycemia in this case but exert their effects via other pathways. It is not entirely surprising because these drugs have different mechanisms of action from that of SFN.

It has been demonstrated that 1% [DCCT (Diabetes Control and Complications Trial) units] decrease of HbA1c corresponds to 37% reduced risk of microvascular complications (*59*). BSE treatment reduced HbA1c from 57.1 mmol/mol (or 7.38%) to 53.4 mmol/mol (or 7.04%) in obese patients with dysregulated T2D. The patients thereby reached the 7% treatment goal recommended by the American Diabetes Association (*60*), which is likely to represent a clinically meaningful effect.

Although the effect of BSE on glucose production was abolished in vitro when the conversion of glucoraphanin to SFN was prevented, we cannot fully determine that SFN explains the effect of BSE given to patients. High doses of BSE cannot yet be recommended to patients as a drug treatment but would require further studies, including data on which groups of patients would potentially benefit most from it. Finally, the findings provide support for using disease signatures based on coexpression networks to interrogate drug signatures, thereby using the large public repositories of gene expression data, as one of many strategies for repurposing compounds of immediate clinical relevance.

MATERIALS AND METHODS

Study design

We first used published gene expression data (*18*) to construct a 50-gene hepatic disease signature and identified SFN as a potential treatment for

excessive hepatic glucose production. We then studied the effects of SFN on the hepatoma cell line H4IIE, primary mouse hepatocytes, and diabetic animal models (Wistar rats and C57BL/6JBomTac and C57BL/6J mice fed a diet with high-fat or high-fructose content). The numbers of independent tests/animals used for each experiment are indicated in the figure legends. Finally, we investigated the effect of SFN-containing BSE in T2D patients in a controlled randomized study with two parallel arms. The predefined inclusion and exclusion criteria for the clinical study are described in the Supplementary Materials and Methods. T2D patients of Scandinavian ethnicity were recruited from the All New Diabetics In Scania (ANDIS) cohort and attended a screening visit, followed by an OGTT 2 weeks later. Placebo or BSE powder was thereafter provided in a double-blind manner as dry mixtures in sealed portion size bags of similar shape and size. Randomization was done using a computer-based block randomization algorithm. After a 12-week treatment period, the patients returned for a final visit including an OGTT. All data analyses were performed with blinded assessment of outcomes. Only patients who had taken >75% of their compound during the total study period and >80% during the last month were included in the analyses. The clinical study was conducted at Skåne University Hospital, Sweden. The study was approved by the Regional Ethics Committee in Lund, and all patients expressed written informed consent. ClinicalTrials.gov Identifier is NCT02801448. For details, see the Supplementary Materials and Methods.

Statistics

Experimental in vitro and animal data were analyzed using Student's *t* test. Additive versus synergistic effects of SFN, metformin, and insulin on glucose production were determined by comparing expected and observed data. Because insulin caused 40% reduction and metformin at 250 μM caused 40% reduction, we would expect 64% reduction if the effects were only additive, whereas the observed reduction was 70% ($P = 0.005$ for expected versus observed effects as shown in Fig. 1B). For the clinical study, the primary effect variables were HbA1c and fasting glucose after versus before the treatment (ΔHbA1c and Δglucose). All analyses were done using one-tailed Student's *t* test between placebo and BSE arms. We also used two-tailed linear regression to compare the relationship between metabolic variables and ΔHbA1c and Δglucose as described in the text.

SUPPLEMENTARY MATERIALS

www.sciencetranslationalmedicine.org/cgi/content/full/9/394/eaah4477/DC1
Materials and Methods
Fig. S1. Effect of SFN on apoptosis, insulin signaling, and OCR in H4IIE cells.
Fig. S2. Effect of SFN on the 50-gene hepatic disease signature.
Fig. S3. Effect of BSE on H4IIE cells and on mice fed an HFD.
Table S1. The 50-gene liver disease signature for T2D.
Table S2. List of compounds used in the analysis (see separate Excel file).
Table S3. Rank order of compounds (see separate Excel file).
Table S4. Expression of enzymes involved in gluconeogenesis.
Table S5. Adverse effects in patients treated with BSE or placebo for 12 weeks.
Table S6. Characteristics of patients discontinuing the study.
References (*61*–*69*)

REFERENCES AND NOTES

1. E. S. Lander, Initial impact of the sequencing of the human genome. *Nature* **470**, 187–197 (2011).
2. J. Lamb, E. D. Crawford, D. Peck, J. W. Modell, I. C. Blat, M. J. Wrobel, J. Lerner, J.-P. Brunet, A. Subramanian, K. N. Ross, M. Reich, H. Hieronymus, G. Wei, S. A. Armstrong, S. J. Haggarty, P. A. Clemons, R. Wei, S. A. Carr, E. S. Lander, T. R. Golub, The Connectivity Map: Using gene-expression signatures to connect small molecules, genes, and disease. *Science* **313**, 1929–1935 (2006).
3. M. Sirota, J. T. Dudley, J. Kim, A. P. Chiang, A. A. Morgan, A. Sweet-Cordero, J. Sage, A. J. Butte, Discovery and preclinical validation of drug indications using compendia of public gene expression data. *Sci. Transl. Med.* **3**, 96ra77 (2011).
4. J. T. Dudley, M. Sirota, M. Shenoy, R. K. Pai, S. Roedder, A. P. Chiang, A. A. Morgan, M. M. Sarwal, P. J. Pasricha, A. J. Butte, Computational repositioning of the anticonvulsant topiramate for inflammatory bowel disease. *Sci. Transl. Med.* **3**, 96ra76 (2011).
5. M. Pulvino, L. Chen, D. Oleksyn, J. Li, G. Compitello, R. Rossi, S. Spence, V. Balakrishnan, C. Jordan, B. Poligone, C. Casulo, R. Burack, J. L. Shapiro, S. Bernstein, J. W. Friedberg, R. J. Deshaies, H. Land, J. Zhao, Inhibition of COP9-signalosome (CSN) deneddylating activity and tumor growth of diffuse large B-cell lymphomas by doxycycline. *Oncotraget* **6**, 14796–14813 (2015).
6. X. Liu, X. Yang, X. Chen, Y. Zhang, X. Pan, G. Wang, Y. Ye, Expression profiling identifies bezafibrate as potential therapeutic drug for lung adenocarcinoma. *J. Cancer* **6**, 1214–1221 (2015).
7. E. Ravasz, A. L. Somera, D. A. Mongru, Z. N. Oltvai, A.-L. Barabasi, Hierarchical organization of modularity in metabolic networks. *Science* **297**, 1551–1555 (2002).
8. T. Mahdi, S. Hänzelmann, A. Salehi, S. J. Muhammed, T. M. Reinbothe, Y. Tang, A. S. Axelsson, Y. Zhou, X. Jing, P. Almgren, U. Krus, J. Taneera, A. M. Blom, V. Lyssenko, J. L. S. Esguerra, O. Hansson, L. Eliasson, J. Derry, E. Zhang, C. B. Wollheim, L. Groop, E. Renström, A. H. Rosengren, Secreted frizzled-related protein 4 reduces insulin secretion and is overexpressed in type 2 diabetes. *Cell Metab.* **16**, 625–633 (2012).
9. B. Zhang, S. Horvath, A general framework for weighted gene co-expression network analysis. *Stat. Appl. Genet. Mol. Biol.* **4**, Article17 (2005).
10. R. A. Defronzo, From the triumvirate to the ominous octet: A new paradigm for the treatment of type 2 diabetes mellitus. *Diabetes* **58**, 773–795 (2009).
11. Global Burden of Disease Study 2013 Collaborators, Global, regional, and national incidence, prevalence, and years lived with disability for 301 acute and chronic diseases and injuries in 188 countries, 1990–2013: A systematic analysis for the Global Burden of Disease Study 2013. *Lancet* **386**, 743–800 (2015).
12. K. Y. Hur, M.-S. Lee, New mechanisms of metformin action: Focusing on mitochondria and the gut. *J. Diabetes Investig.* **6**, 600–609 (2015).
13. R. A. Miller, Q. Chu, J. Xie, M. Foretz, B. Viollet, M. J. Birnbaum, Biguanides suppress hepatic glucagon signalling by decreasing production of cyclic AMP. *Nature* **494**, 256–260 (2013).
14. A. K. Madiraju, D. M. Erion, Y. Rahimi, X.-M. Zhang, D. T. Braddock, R. A. Albright, B. J. Prigaro, J. L. Wood, S. Bhanot, M. J. MacDonald, M. J. Jurczak, J.-P. Camporez, H.-Y. Lee, G. W. Cline, V. T. Samuel, R. G. Kibbey, G. I. Shulman, Metformin suppresses gluconeogenesis by inhibiting mitochondrial glycerophosphate dehydrogenase. *Nature* **510**, 542–546 (2014).
15. A. Solini, G. Penno, E. Bonora, C. Fondelli, E. Orsi, R. Trevisan, M. Vedovato, F. Cavalot, M. Cignarelli, S. Morano, E. Ferrannini, G. Pugliese;Renal Insuffieciency and Cardiovascular events Study Group, Age, renal dysfunction, cardiovascular disease, and antihyperglycemic treatment in type 2 diabetes mellitus: Findings from the Renal Insufficiency and Cardiovascular Events Italian Multicenter Study. *J. Am. Geriatr. Soc.* **61**, 1253–1261 (2013).
16. A. J. Garber, T. G. Duncan, A. M. Goodman, D. J. Mills, J. L. Rohlf, Efficacy of metformin in type II diabetes: Results of a double-blind, placebo-controlled, dose-response trial. *Am. J. Med.* **103**, 491–497 (1997).
17. Y. Chen, J. Zhu, P. Y. Lum, X. Yang, S. Pinto, D. J. MacNeil, C. Zhang, J. Lamb, S. Edwards, S. K. Sieberts, A. Leonardson, L. W. Castellini, S. Wang, M.-F. Champy, B. Zhang, V. Emilsson, S. Doss, A. Ghazalpour, S. Horvath, T. A. Drake, A. J. Lusis, E. E. Schadt, Variations in DNA elucidate molecular networks that cause disease. *Nature* **452**, 429–435 (2008).
18. S. Wang, N. Yehya, E. E. Schadt, H. Wang, T. A. Drake, A. J. Lusis, Genetic and genomic analysis of a fat mass trait with complex inheritance reveals marked sex specificity. *PLOS Genet.* **2**, e15 (2006).
19. B. Zhang, C. Gaiteri, L.-G. Bodea, Z. Wang, J. McElwee, A. A. Podtelezhnikov, C. Zhang, T. Xie, L. Tran, R. Dobrin, E. Fluder, B. Clurman, S. Melquist, M. Narayanan, C. Suver, H. Shah, M. Mahajan, T. Gillis, J. Mysore, M. E. MacDonald, J. R. Lamb, D. A. Bennett, C. Molony, D. J. Stone, V. Gudnason, A. J. Myers, E. E. Schadt, H. Neumann, J. Zhu, V. Emilsson, Integrated systems approach identifies genetic nodes and networks in late-onset Alzheimer's disease. *Cell* **153**, 707–720 (2013).
20. M. I. McCarthy, Genomics, type 2 diabetes, and obesity. *N. Engl. J. Med.* **363**, 2339–2350 (2010).
21. V. Emilsson, G. Thorleifsson, B. Zhang, A. S. Leonardson, F. Zink, J. Zhu, S. Carlson, A. Helgason, G. B. Walters, S. Gunnarsdottir, M. Mouy, V. Steinthorsdottir, G. H. Eiriksdottir, G. Bjornsdottir, I. Reynisdottir, D. Gudbjartsson, A. Helgadottir, A. Jonasdottir, U. Styrkarsdottir, S. Gretarsdottir, K. P. Magnusson, H. Stefansson, R. Fossdal, K. Kristjansson, H. G. Gislason, T. Stefansson, B. G. Leifsson, U. Thorsteinsdottir, J. R. Lamb, J. R. Gulcher, M. L. Reitman, A. Kong, E. E. Schadt, K. Stefansson, Genetics of gene expression and its effect on disease. *Nature* **452**, 423–428 (2008).

22. K. Gross-Steinmeyer, P. L. Stapleton, J. H. Tracy, T. K. Bammler, S. C. Strom, D. L. Eaton, Sulforaphane- and phenethyl isothiocyanate–induced inhibition of aflatoxin B1–mediated genotoxicity in human hepatocytes: Role of GSTM1 genotype and CYP3A4 gene expression. *Toxicol. Sci.* **116**, 422–432 (2010).
23. K. Itoh, T. Chiba, S. Takahashi, T. Ishii, K. Igarashi, Y. Katoh, T. Oyake, N. Hayashi, K. Satoh, I. Hatayama, M. Yamamoto, Y.-i. Nabeshima, An Nrf2/small Maf heterodimer mediates the induction of phase II detoxifying enzyme genes through antioxidant response elements. *Biochem. Biophys. Res. Commun.* **236**, 313–322 (1997).
24. B. R. Imhoff, J. M. Hansen, Extracellular redox status regulates Nrf2 activation through mitochondrial reactive oxygen species. *Biochem. J.* **424**, 491–500 (2009).
25. Y. Zhang, P. Talalay, C. G. Cho, G. H. Posner, A major inducer of anticarcinogenic protective enzymes from broccoli: Isolation and elucidation of structure. *Proc. Natl. Acad. Sci. U.S.A.* **89**, 2399–2403 (1992).
26. L. Wu, M. H. Noyan Ashraf, M. Facci, R. Wang, P. G. Paterson, A. Ferrie, B. H. Juurlink, Dietary approach to attenuate oxidative stress, hypertension, and inflammation in the cardiovascular system. *Proc. Natl. Acad. Sci. U.S.A.* **101**, 7094–7099 (2004).
27. H. Y. Kay, W. D. Kim, S. J. Hwang, H.-S. Choi, R. K. Gilroy, Y.-J. Wan, S. G. Kim, Nrf2 inhibits LXRα-dependent hepatic lipogenesis by competing with FXR for acetylase binding. *Antioxid. Redox Signal.* **15**, 2135–2146 (2011).
28. G. Yang, H. E. Lee, J. Y. Lee, A pharmacological inhibitor of NLRP3 inflammasome prevents non-alcoholic fatty liver disease in a mouse model induced by high fat diet. *Sci. Rep.* **6**, 24399 (2016).
29. D. Gao, S. Nong, X. Huang, Y. Lu, H. Zhao, Y. Lin, Y. Man, S. Wang, J. Yang, J. Li, The effects of palmitate on hepatic insulin resistance are mediated by NADPH oxidase 3-derived reactive oxygen species through JNK and $p38^{MAPK}$ pathways. *J. Biol. Chem.* **285**, 29965–29973 (2010).
30. S. A. Blumenthal, Stimulation of gluconeogenesis by palmitic acid in rat hepatocytes: Evidence that this effect can be dissociated from the provision of reducing equivalents. *Metabolism* **32**, 971–976 (1983).
31. K. Itoh, N. Wakabayashi, Y. Katoh, T. Ishii, K. Igarashi, J. D. Engel, M. Yamamoto, Keap1 represses nuclear activation of antioxidant responsive elements by Nrf2 through binding to the amino-terminal Neh2 domain. *Genes Dev.* **13**, 76–86 (1999).
32. A. T. Dinkova-Kostova, A. Y. Abramov, The emerging role of Nrf2 in mitochondrial function. *Free Radic. Biol. Med.* **88**, 179–188 (2015).
33. R. W. Hanson, L. Reshef, Regulation of phosphoenolpyruvate carboxykinase (GTP) gene expression. *Annu. Rev. Biochem.* **66**, 581–611 (1997).
34. A. Gastaldelli, S. Baldi, M. Pettiti, E. Toschi, S. Camastra, A. Natali, B. R. Landau, E. Ferrannini, Influence of obesity and type 2 diabetes on gluconeogenesis and glucose output in humans: A quantitative study. *Diabetes* **49**, 1367–1373 (2000).
35. M. Roden, H. Stingl, V. Chandramouli, W. C. Schumann, A. Hofer, B. R. Landau, P. Nowotny, W. Waldhäusl, G. I. Shulman, Effects of free fatty acid elevation on postabsorptive endogenous glucose production and gluconeogenesis in humans. *Diabetes* **49**, 701–707 (2000).
36. A. Gastaldelli, Y. Miyazaki, M. Pettiti, E. Buzzigoli, S. Mahankali, E. Ferrannini, R. A. DeFronzo, Separate contribution of diabetes, total fat mass, and fat topography to glucose production, gluconeogenesis, and glycogenolysis. *J. Clin. Endocrinol. Metab.* **89**, 3914–3921 (2004).
37. L. Ye, A. T. Dinkova-Kostova, K. L. Wade, Y. Zhang, T. A. Shapiro, P. Talalay, Quantitative determination of dithiocarbamates in human plasma, serum, erythrocytes and urine: Pharmacokinetics of broccoli sprout isothiocyanates in humans. *Clin. Chim. Acta* **316**, 43–53 (2002).
38. T. A. Shapiro, J. W. Fahey, K. L. Wade, K. K. Stephenson, P. Talalay, Chemoprotective glucosinolates and isothiocyanates of broccoli sprouts: Metabolism and excretion in humans. *Cancer* **10**, 501–508 (2001).
39. T. A. Shapiro, J. W. Fahey, K. L. Wade, K. K. Stephenson, P. Talalay, Human metabolism and excretion of cancer chemoprotective glucosinolates and isothiocyanates of cruciferous vegetables. *Cancer Epidemiol. Biomarkers Prev.* **7**, 1091–1100 (1998).
40. J. W. Fahey, W. D. Holtzclaw, S. L. Wehage, K. L. Wade, K. K. Stephenson, P. Talalay, Sulforaphane bioavailability from glucoraphanin-rich broccoli: Control by active endogenous myrosinase. *PLOS ONE* **10**, e0140963 (2015).
41. R. Hu, V. Hebbar, B.-R. Kim, C. Chen, B. Winnik, B. Buckley, P. Soteropoulos, P. Tolias, R. P. Hart, A.-N. Kong, In vivo pharmacokinetics and regulation of gene expression profiles by isothiocyanate sulforaphane in the rat. *J. Pharmacol. Exp. Ther.* **310**, 263–271 (2004).
42. T. W. Kensler, J.-G. Chen, P. A. Egner, J. W. Fahey, L. P. Jacobson, K. K. Stephenson, L. Ye, J. L. Coady, J.-B. Wang, Y. Wu, Y. Sun, Q.-N. Zhang, B.-C. Zhang, Y.-R. Zhu, G.-S. Qian, S. G. Carmella, S. S. Hecht, L. Benning, S. J. Gange, J. D. Groopman, P. Talalay, Effects of glucosinolate-rich broccoli sprouts on urinary levels of aflatoxin-DNA adducts and phenanthrene tetraols in a randomized clinical trial in He Zuo township, Qidong, People's Republic of China. *Cancer Epidemiol. Biomarkers Prev.* **14**, 2605–2613 (2005).
43. T. A. Shapiro, J. W. Fahey, A. T. Dinkova-Kostova, W. D. Holtzclaw, K. K. Stephenson, K. L. Wade, L. Ye, P. Talalay, Safety, tolerance, and metabolism of broccoli sprout glucosinolates and isothiocyanates: A clinical phase I study. *Nutr. Cancer* **55**, 53–62 (2006).
44. R. H. Brown, C. Reynolds, A. Brooker, P. Talalay, J. W. Fahey, Sulforaphane improves the bronchoprotective response in asthmatics through Nrf2-mediated gene pathways. *Respir. Res.* **16**, 106 (2015).
45. K. Singh, S. L. Connors, E. A. Macklin, K. D. Smith, J. W. Fahey, P. Talalay, A. W. Zimmerman, Sulforaphane treatment of autism spectrum disorder (ASD). *Proc. Natl. Acad. Sci. U.S.A.* **111**, 15550–15555 (2014).
46. D. Van Eylen, I. Oey, M. Hendrickx, A. Van Loey, Kinetics of the stability of broccoli (*Brassica oleracea* Cv. Italica) myrosinase and isothiocyanates in broccoli juice during pressure/temperature treatments. *J. Agric. Food Chem.* **55**, 2163–2170 (2007).
47. R. A. DeFronzo, E. Ferrannini, D. C. Simonson, Fasting hyperglycemia in non-insulin-dependent diabetes mellitus: Contributions of excessive hepatic glucose production and impaired tissue glucose uptake. *Metabolism* **38**, 387–395 (1989).
48. A. Gastaldelli, M. Kozakova, K. Højlund, A. Flyvbjerg, A. Favuzzi, A. Mitrakou, B. Balkau, Fatty liver is associated with insulin resistance, risk of coronary heart disease, and early atherosclerosis in a large European population. *Hepatology* **49**, 1537–1544 (2009).
49. G. Negi, A. Kumar, S. S. Sharma, Nrf2 and NF-κB modulation by sulforaphane counteracts multiple manifestations of diabetic neuropathy in rats and high glucose-induced changes. *Curr. Neurovasc. Res.* **8**, 294–304 (2011).
50. H. Zheng, S. A. Whitman, W. Wu, G. T. Wondrak, P. K. Wong, D. Fang, D. D. Zhang, Therapeutic potential of Nrf2 activators in streptozotocin-induced diabetic nephropathy. *Diabetes* **60**, 3055–3066 (2011).
51. M. Xue, Q. Qian, A. Adaikalakoteswari, N. Rabbani, R. Babaei-Jadidi, P. J. Thornalley, Activation of NF-E2–related factor-2 reverses biochemical dysfunction of endothelial cells induced by hyperglycemia linked to vascular disease. *Diabetes* **57**, 2809–2817 (2008).
52. X. Miao, Y. Bai, W. Sun, W. Cui, Y. Xin, Y. Wang, Y. Tan, L. Miao, Y. Fu, G. Su, L. Cai, Sulforaphane prevention of diabetes-induced aortic damage was associated with the up-regulation of Nrf2 and its down-stream antioxidants. *Nutr. Metab.* **9**, 84 (2012).
53. E. M. Harrison, S. J. McNally, L. Devey, O. J. Garden, J. A. Ross, S. J. Wigmore, Insulin induces heme oxygenase-1 through the phosphatidylinositol 3-kinase/Akt pathway and the Nrf2 transcription factor in renal cells. *FEBS J.* **273**, 2345–2356 (2006).
54. Y. Tan, T. Ichikawa, J. Li, Q. Si, H. Yang, X. Chen, C. S. Goldblatt, C. J. Meyer, X. Li, L. Cai, T. Cui, Diabetic downregulation of Nrf2 activity via ERK contributes to oxidative stress–induced insulin resistance in cardiac cells in vitro and in vivo. *Diabetes* **60**, 625–633 (2011).
55. Z. Yu, W. Shao, Y. Chiang, W. Foltz, Z. Zhang, W. Ling, I. G. Fantus, T. Jin, Oltipraz upregulates the nuclear factor 2 alpha subunit (NRF2) antioxidant system and prevents insulin resistance and obesity induced by a high-fat diet in C57BL/6J mice. *Diabetologia* **54**, 922–934 (2011).
56. A. Uruno, Y. Furusawa, Y. Yagishita, T. Fukutomi, H. Muramatsu, T. Negishi, A. Sugawara, T. W. Kensler, M. Yamamoto, The Keap1-Nrf2 system prevents onset of diabetes mellitus. *Mol. Cell Biol.* **33**, 2996–3010 (2013).
57. R. A. Rizza, Pathogenesis of fasting and postprandial hyperglycemia in type 2 diabetes: Implications for therapy. *Diabetes* **59**, 2697–2707 (2010).
58. M.-Y. Song, E.-K. Kim, W.-S. Moon, J.-W. Park, H.-J. Kim, H.-S. So, R. Park, K.-B. Kwon, B.-H. Park, Sulforaphane protects against cytokine- and streptozotocin-induced β-cell damage by suppressing the NF-κB pathway. *Toxicol. Appl. Pharmacol.* **235**, 57–67 (2009).
59. I. M. Stratton, A. I. Adler, H. A. Neil, D. R. Matthews, S. E. Manley, C. A. Cull, D. Hadden, R. C. Turner, R. R. Holman, Association of glycaemia with macrovascular and microvascular complications of type 2 diabetes (UKPDS 35): Prospective observational study. *BMJ* **321**, 405–412 (2000).
60. Standards of medical care in diabetes—2016: Summary of revisions. *Diabetes Care* **39** (suppl. 1), S4–S5 (2016).
61. P. Langfelder, S. Horvath, WGCNA: An R package for weighted correlation network analysis. *BMC Bioinformatics* **9**, 559 (2008).
62. B. Snel, G. Lehmann, P. Bork, M. A. Huynen, STRING: A web-server to retrieve and display the repeatedly occurring neighbourhood of a gene. *Nucleic Acids Res.* **28**, 3442–3444 (2000).
63. S. P. Cousin, S. R. Hügl, C. E. Wrede, H. Kajio, M. G. Myers Jr., C. J. Rhodes, Free fatty acid-induced inhibition of glucose and insulin-like growth factor I-induced deoxyribonucleic acid synthesis in the pancreatic β-cell line INS-1. *Endocrinology* **142**, 229–240 (2001).
64. S. Malmgren, D. G. Nicholls, J. Taneera, K. Bacos, T. Koeck, A. Tamaddon, R. Wibom, L. Groop, C. Ling, H. Mulder, V. V. Sharoyko, Tight coupling between glucose and mitochondrial metabolism in clonal β-cells is required for robust insulin secretion. *J. Biol. Chem.* **284**, 32395–32404 (2009).
65. M. D. Brand, D. G. Nicholls, Assessing mitochondrial dysfunction in cells. *Biochem. J.* **435**, 297–312 (2011).
66. D. M. Bier, R. D. Leake, M. W. Haymond, K. J. Arnold, L. D. Gruenke, M. A. Sperling, D. M. Kipnis, Measurement of "true" glucose production rates in infancy and childhood with 6,6-dideuteroglucose. *Diabetes* **26**, 1016–1023 (1977).

67. S. K. Chacko, A. L. Sunehag, Gluconeogenesis continues in premature infants receiving total parenteral nutrition. *Arch. Dis. Child. Fetal Neonatal Ed.* **95**, F413–F418 (2010).
68. S. K. Chacko, A. L. Sunehag, S. Sharma, P. J. J. Sauer, M. W. Haymond, Measurement of gluconeogenesis using glucose fragments and mass spectrometry after ingestion of deuterium oxide. *J. Appl. Physiol.* **104**, 944–951 (2008).
69. E. Schwarze, H. Tolleshaug, O. Seglen, Uptake and degradation of asialo-orosomucoid in hepatocytes from carcinogen-treated rats. *Carcinogenesis* **6**, 777–782 (1985).

Acknowledgments: We thank M. Fälemark and H. Ferm, who were responsible research nurses, as well as J. M. Odeberg, K. Hansson, K. Elofsson, G. P. Samuelsson, and M. A. Ohlsson at the Clinical Trial Unit Skåne University Hospital for conducting the clinical trial. We thank B.-M. Nilsson and A.-M. V. Ramsay for the expert technical assistance. We thank A.-H. T. Fischer of Timeline Bioresearch for the expert assistance with clamp experiments. We also thank L. Groop and colleagues at ANDIS, from which the patients were recruited. This work is in part a publication of the U.S. Department of Agriculture/Agricultural Research Service, Children's Nutrition Research Center, Department of Pediatrics, Baylor College of Medicine, Houston, TX. The contents of this publication do not necessarily reflect the views or policies of the U.S. Department of Agriculture, and mention of trade names, commercial products, or organizations does not imply endorsement from the U.S. government. **Funding:** The study was supported by the Ragnar Söderberg Foundation, the Swedish Foundation for Strategic Research, Lantmännen Research Foundation, the NovoNordisk Foundation, ALF Region Skåne, the Hjelt Foundation, the Lewis B. and Dorothy Cullman Foundation, and Knut and Alice Wallenberg's foundation via the Wallenberg Centre for Molecular and Translational Medicine in Gothenburg.
Author contributions: A.S.A., J.M.J.D., J.W.F., C.B.W., N.W., S.H.F., H.M., and A.H.R. designed the study. A.S.A., E.T., Y.T., and H.A.N. performed the experiments. A.H.R., B.M., and J.M.J.D. analyzed the network data. A.S.A., E.T., and A.H.R. analyzed the experimental data. M.W.H. and S.C. designed and analyzed the gluconeogenesis measurements. A.H.R. designed the clinical trial. A.S.A. and A.H.R. wrote the paper. All authors commented on the manuscript. **Competing interests:** A.S.A. and A.H.R. are inventors on patent applications (SE1251306-5, US9,597,307B2, and EU2919775) submitted by Lund University that cover the use of SFN to treat exaggerated hepatic glucose production. The rights to use this patent have been licensed to Lantmännen AB, an agricultural cooperative owned by Swedish farmers. Lantmännen AB provided the BSE and placebo for the study, and Lantmännen Research Fund financed part of the study. However, this academic investigation was sponsored by Lund University, and Lantmännen AB had no influence on the study procedures, data analysis, or interpretation of the data in the manuscript. All other authors declare that they have no competing interests. **Data and materials availability:** Clinical Trials.gov Identifier is NCT02801448 (https://clinicaltrials.gov/ct2/results?term=NCT02801448&Search=Search). The liver gene expression data are available in the GEO database (accession number GSE2814). All raw data are freely available from the authors upon request.

Submitted 28 June 2016
Resubmitted 23 February 2017
Accepted 5 May 2017
Published 14 June 2017
10.1126/scitranslmed.aah4477

Citation: A. S. Axelsson, E. Tubbs, B. Mecham, S. Chacko, H. A. Nenonen, Y. Tang, J. W. Fahey, J. M. J. Derry, C. B. Wollheim, N. Wierup, M. W. Haymond, S. H. Friend, H. Mulder, A. H. Rosengren, Sulforaphane reduces hepatic glucose production and improves glucose control in patients with type 2 diabetes. *Sci. Transl. Med.* **9**, eaah4477 (2017).

Science Translational Medicine

Sulforaphane reduces hepatic glucose production and improves glucose control in patients with type 2 diabetes

Annika S. Axelsson, Emily Tubbs, Brig Mecham, Shaji Chacko, Hannah A. Nenonen, Yunzhao Tang, Jed W. Fahey, Jonathan M. J. Derry, Claes B. Wollheim, Nils Wierup, Morey W. Haymond, Stephen H. Friend, Hindrik Mulder and Anders H. Rosengren

Sci Transl Med **9**, eaah4477.
DOI: 10.1126/scitranslmed.aah4477

Another reason to eat your broccoli

Type 2 diabetes is becoming increasingly common worldwide, and not all patients can be successfully treated with the existing drugs. Axelsson *et al*. analyzed the pattern of gene expression associated with type 2 diabetes and compared it to the gene signatures for thousands of drug candidates to find compounds that could counteract the effects of diabetes. The leading candidate from this analysis was sulforaphane, a natural compound found in broccoli and other vegetables. The authors showed that sulforaphane inhibits glucose production in cultured cells and improves glucose tolerance in rodents on high-fat or high-fructose diets. Moreover, in a clinical trial, sulforaphane-containing broccoli sprout extract was well tolerated and improved fasting glucose in human patients with obesity and dysregulated type 2 diabetes.

Science Translational Medicine
AAAS

www.sciencetranslationalmedicine.org/cgi/content/full/9/394/eaah4477/DC1

Supplementary Materials for

Sulforaphane reduces hepatic glucose production and improves glucose control in patients with type 2 diabetes

Annika S. Axelsson, Emily Tubbs, Brig Mecham, Shaji Chacko, Hannah A. Nenonen, Yunzhao Tang, Jed W. Fahey, Jonathan M. J. Derry, Claes B. Wollheim, Nils Wierup, Morey W. Haymond, Stephen H. Friend, Hindrik Mulder, Anders H. Rosengren*

*Corresponding author. Email: anders.rosengren@gu.se

Published 14 June 2017, *Sci. Transl. Med.* **9**, eaah4477 (2017)
DOI: 10.1126/scitranslmed.aah4477

The PDF file includes:

Other Supplementary Material for this manuscript includes the following:
(available at
www.sciencetranslationalmedicine.org/cgi/content/full/9/394/eaah4477/DC1)

Supplementary Materials and Methods

Bioinformatics

Generation of the disease signature. C57BL/6J ApoE-/- mice were purchased from Jackson Laboratory. C3H/HeJ ApoE-/- mice were generated by backcrossing C57BL/6J ApoE-/- to C3H/HeJ mice for ten generations. An F2 intercross with a total of 334 mice (169 female, 165 male) was then generated between C57BL/6J ApoE-/- and C3H/HeJ ApoE-/- mice.

All mice were fed Purina Chow containing 4% fat until 8 weeks of age and then transferred to a "Western" diet containing 42% fat and 0.15% cholesterol for 16 weeks. Mice were sacrificed at 24 weeks of age. Tissues were immediately collected and flash-frozen in liquid nitrogen. This cross, termed the B × H cross, was designed to recapitulate a range of phenotypes associated with the metabolic syndrome (*17, 18*).

RNA preparation and array hybridizations were done at Rosetta Inpharmatics using custom inkjet microarrays manufactured by Agilent Technologies. The microarrays consisted of 2186 control probes and 23,574 gene probes extracted from mouse Unigene clusters and combined with RefSeq sequences and RIKEN full-length cDNA clones. The liver expression data have previously been deposited into the GEO database (accession number GSE2814).

Based on log2-transformed microarray expression data from liver samples of the 334 mice in the B × H cross (GSE2814 in GEO), co-expression network analysis was performed in R (version 2.15.1) . Using the weighted gene co-expression network analysis (WGCNA) framework (*9*) and the corresponding Bioconductor package (*61*), we first calculated the pair-wise co-expression for all genes and formed a similarity matrix based on the Pearson correlation coefficients $s_{i,j} = |cor(x_i,x_j)|$, where x_i denotes the expression vector for gene i across the samples.

Next, the similarity matrix was transformed into an adjacency matrix $a_{i,j} = |cor(x_i,x_j)|^{\beta}$. The connectivity of a gene in a network (the degree *k*) equals the sum of all connections for that gene.

Biological networks have been suggested to exhibit a scale-free property (*7*), which means that the probability that a node is connected with k other nodes (the degree distribution p(*k*)) decays as a power function $p(k) \sim k^{-\gamma}$. Linear regression analysis of log-transformed *k* and p(*k*) was used to estimate how well the co-expression network satisfied the scale-free topology for different values of β. Based on the adjacency matrix, the topological overlap, which reflects the relative gene interconnectedness, was calculated for all gene pairs (*7*). The non-negative and symmetric topological overlap matrix $\Omega = [\omega_{i,j}]$ was converted to dissimilarity (distance) measures $d_{i,j} = 1-\omega_{i,j}$, which were used for module identification. The eigengene, defined as the 1st principal component of the gene expression matrix, was determined for each module and was correlated with the phenotype traits. In this way we identified groups of co-expressed genes ('modules'), including a total of 1720 genes which were associated with hyperglycemia.

We used four criterion variables to select those of the 1720 genes that were most likely to be involved in diabetes pathophysiology.

1) For each gene in the T2D-associated module, the connectivity within the module (k_{in}), which equals the sum of all connections for that gene, was determined using the weighted gene co-expression network analysis (WGCNA) framework (*9*) and the corresponding Bioconductor package (*61*).

2) Key regulators were identified based on Bayesian modelling using the methodology described in (*19*).

3) Information on genetic risk variants associated with T2D was used to construct a protein-protein interaction network with a total of 319 genes centered on those that are in close proximity of known T2D risk variants (*20*). We used the String platform (*62*), including proteins directly connected (1 edge) to T2D risk genes and a cut-off of 0.4.

4) We used data on single nucleotide polymorphisms associated with gene expression traits (eSNPs) in human liver samples to identify genes with eSNPs that were also risk variants for T2D, because such genes have been suggested to cause metabolic disease (*21*).

A leave-one-out approach was then applied to impute weights for each of these four criterion variables. We used linear modeling $c_1 = \beta_2 c_2 + \beta_3 c_3 + \beta_4 c_4$, in which each criterion variable was predicted by the others across the genes. The leave-one-out approach was iterated for each of the criterion variables c_1, c_2, c_3, c_4. The β coefficients (β_1, β_2, β_3, and β_4) were obtained by solving the resultant equation system. The average of the β coefficients across all genes was then used as a weight for each criterion variable. In this way, a sum score was computed for each of the 1720 genes based on the four variables and their weights to filter out those genes which best met the criteria. This leave-one-out procedure enabled us to analyze the relative importance of each variable in order to incorporate the relative weight of each variable in the final sum score. We used the R software for this approach. The relative contribution of each criterion to the ranking was 69% for criterion 1, 21% for criterion 2, 3% for criterion 3, and 7% for criterion 4, as determined by linear regression.

We assumed that genes with the highest sum score would incorporate the most pathophysiological information and therefore generated a final disease signature, representing genes with a sum score above 2 standard deviations from the mean and composed of the 25 genes with the highest score that were overexpressed in diseased tissues relative to controls and the 25 genes with the highest score that were downregulated in disease.

Comparisons with drug signatures. Gene expression profiles from 3852 publically available microarray data sets (www.ncbi.nlm.nih.gov/geo and https://www.ebi.ac.uk/arrayexpress/) based on experiments with compound treatments of cell lines or primary tissues and analyzed by Affymetrix, Agilent, or Illumina chips were downloaded and processed. Only data sets for which the full raw data were available were included. A list of all compounds is available in table S2, and all raw data are freely available upon request. The probe-level data were processed using the Supervised Normalization of Microarrays (SNM) framework to normalize for array effects, detect and remove outlier arrays, and facilitate cross-dataset analysis. Our specific implementation of this framework was as follows: 1) for each array we calculated the average value of all probes aligning to gene g; 2) we defined an overall average for gene g across all microarrays from that platform; 3) for every sample, we used a b-spline basis function to remove any intensity-dependent variation between the gene-level mean values calculated in step 1 with the average values calculated in step 2 as the reference.

Next, summary statistics were calculated for each gene in each study. These statistics were then aggregated into matrices where each row corresponds to a gene, each column a study, and each element a summary statistic (mean or variance). We used a Kolmogorov-Smirnov test to compare the disease signature with the drug signatures. After the Kolmogorov-Smirnov test, we applied an enrichment test as used in Connectivity Map (*2*), performing 1000 permutations to correct for data sets containing multiple profiles of the same compound, concentration, and tissue. The resulting enrichment metric was used to rank-order compounds for their potential ability to reverse the hepatic disease signature.

In vitro experiments

H4IIE cell culture. Rat hepatoma cells H4IIE (ATCC) were cultured in EMEM (ATCC) with the addition of 10% FBS, 100 IU/ml penicillin, and 100 μg/ml streptomycin at 37°C, 5% CO_2.

Palmitate for cell culture. Palmitate (Sigma-Aldrich) was conjugated to essentially fatty acid-free BSA (Sigma-Aldrich) as described by Cousin et al. (*63*).

Glucose production assay (GPA). H4IIE cells were seeded at 100 000 or 210 000 cells/well in 24-well plates, and GPA was performed on confluent cells (72 or 48 hours after seeding, respectively). Sulforaphane (LKT laboratories), metformin (Sigma-Aldrich), broccoli sprout extract (from portion packages used for the patient study; see below), or placebo (see below) was added to the cells 24 hours before the GPA. For the GPA, cells were washed 3 times with glucose production buffer (118 mM NaCl, 4.7 mM KCl, 1.2 mM $MgSO_4$, 1.2 mM KH_2PO_4, 1.2 mM $CaCl_2$, 20 mM $NaHCO_3$, 25 mM HEPES, 20 mM L-lactate, 2 mM pyruvate, 10 mM L-glutamine, and 0.025% BSA; pH 7.4) and 350 µl of buffer with or without 10 nM insulin (Actrapid Penfill, Novo Nordisk) was added. The cells were incubated at 37°C, 5% CO_2 for 5 hours. They were then put on ice, and 250 µl of buffer was removed for glucose measurements. The cells were washed once with cold PBS and lysed with RIPA buffer (50 mM Tris HCl pH 8, 150 mM NaCl, 1% NP-40/Triton X, 0.1% SDS, 0.5% sodium deoxycholate, 2 mM EDTA, 50 mM NaF) for determination of protein content. The buffer samples were centrifuged for 5 min at 500 x g and the supernatant transferred to a new tube. Glucose concentration was determined using the AmplexRed Glucose/Glucose Oxidase Assay Kit (LifeTechnologies). The cell lysates were centrifuged for 10 min at 12 000 x g at 4°C, and protein content in the supernatant was measured using Pierce BCA Protein Assay Kit (ThermoScientific).

RNA interference. Cells were transfected with siRNA using DharmaFECT 1 (ThermoFischer) according to the manufacturer's description, using EMEM without additives for transfection complex formation and antibiotic-free medium for transfection. The following siRNAs were used: all Silencer Select siRNAs from ThermoFischer: Negative Control no.2, Nfe2l2 s136129, and Pck1 s168849. For NRF2 silencing, cells were transfected with 60 nM siRNA at seeding, the medium was changed after 24 hours, and assays performed after 72 hours. For PCK1 silencing, cells were transfected with 50 nM siRNA at seeding and then transfected again with 50 nM siRNA 24 hours after seeding. Assays were performed 72 hours after the first transfection. Transfection efficiency was assessed by qRT-PCR as described below.

RNA isolation and qRT-PCR. RNA from H4IIE cells for qRT-PCR analysis was isolated using the RNeasy Plus kit (Qiagen). Reverse transcription was performed using SuperScript VILO cDNA synthesis kit (ThermoFisher). Quantitative RT-PCR was performed on a ViiA 7 Real-Time PCR System (Life Technologies) or a QuantStudio 7 Flex Real-Time PCR System (Life Technologies) using TaqMan Gene Expression Assays and TaqMan Universal PCR Master Mix (ThermoFisher). Relative gene expression was measured from triplicate average Cq values normalized to the geometric mean of *Hprt1*, *B2m*, and *Polr2a* Cq values.

Microarray analysis of rat liver and H4IIE cells. Rat liver samples for microarray analysis were homogenized in Qiazol reagent (Qiagen) using a TissueLyser II (Qiagen), and total RNA was extracted using the mRNeasy kit (Qiagen). RNA quality and concentration were measured using an Agilent 2100 Bioanalyzer (Bio-Rad) and a Nanodrop ND-1000 (NanoDrop Technologies). Agilent rat microarray chips were used for gene expression analysis in accordance with the standard protocol.

Preparation of nuclear extracts. Nuclear cell fractions from H4IIE cells transfected with Nrf2 siRNA and treated with 3 µM SFN for 24 hours were extracted using the NE-PER Nuclear and Cytoplasmic Extraction Reagents (ThermoFisher). Purity of the nuclear fractions was tested using nucleoporin p62 (NUP62; nucleus-specific) and superoxide dismutase 4 (SOD4; cytoplasm-specific) antibodies. The SOD4 content in the nuclear extracts was less than 0.5% of that of the cytoplasmic extracts.

Western blot. H4IIE cells were washed once with ice-cold PBS and then lysed with RIPA buffer (50 mM Tris HCl, 150 mM NaCl, 1% NP-40/Triton X, 0.1% SDS, 0.5% sodium deoxycholate, 2 mM EDTA, 50 mM NaF) supplemented with protease inhibitor (Complete, Roche). Samples were kept on ice and lightly shaken until cells were detached. The lysate was collected and centrifuged at 10 000 x g for 10 min. The supernatant was either stored at -80°C or used directly for analysis. A defined amount of protein (15-30 µg) was loaded per well and separated on 10% or 4-15% Mini-PROTEAN TGX precast regular or Stain-Free polyacrylamide gels (Bio-Rad). Proteins were transferred to a PVDF membrane (GE Healthcare) at 350 mA for 1.5 hours using regular transfer buffer (58 mM

Tris, 186 mM glycine, 0.1% SDS, 20% ethanol) under cooling conditions. Blocking of the membrane and incubation with antibodies were performed in TBST with 5% milk, except for incubation with anti-phosphosite antibodies which was performed in TBST with 5% BSA. Stain-Free gels were activated with UV light for 1 min before transfer to produce tryptophan-dependent fluorescence, and total protein on the membrane after transfer was analyzed before blocking with milk. Primary antibodies used were against NRF2 (polyclonal from Abcam, ab137550, diluted 1:1000), nucleoporin p62 (monoclonal from BD Biosciences, 610497, diluted 1:1000), superoxide dismutase 4 (monoclonal from Abcam, ab137131, diluted 1:1000), PCK1 (polyclonal from Abcam, ab70358, diluted to 1 µg/ml), phospho-IRS1 pTyr612 (polyclonal from ThermoFisher, 44-816G, diluted 1:500) and phospho-AKT pSer473 (monoclonal from ThermoFisher, 44-621G, diluted 1:500). Incubation with primary antibodies was performed overnight at 4°C. Secondary HRP-linked antibodies used were anti-rabbit (Cell Systems, diluted 1:2000) and anti-mouse (Dako, diluted 1:2000). Incubation with secondary antibodies was performed overnight at 4°C or for 2 hours at room temperature. SuperSignal West Pico Chemiluminescent Substrate or SuperSignal West Femto Maximum Sensitivity Substrate (ThermoFischer) was used for visualization of proteins with a ChemiDoc XRS+ System (Bio-Rad). The intensity of each protein band was normalized to the intensity of nucleoporin p62 for nuclear extracts or to the total protein in the lane when using Stain-Free gels and blots.

Mitochondria spare respiratory capacity measurements. Oxygen consumption rates (OCR) were measured by the XF24 Extracellular Flux Analyzer (Seahorse Bioscience) as previously described (*64*). H4IIE cells were seeded onto poly-D-lysine coated XF24 24-well plates at 40 000 cells/well 48 hours before the assay and incubated with 3 µM SFN 24 hours before the assay. The cells were pre-incubated in 500 µl assay buffer, the same buffer as used for the glucose production assay (118 mM NaCl, 4.7 mM KCl, 1.2 mM $MgSO_4$, 1.2 mM KH_2PO_4, 1.2 mM $CaCl_2$, 20 mM $NaHCO_3$, 25 mM HEPES, 20 mM L-lactate, 2 mM pyruvate, 10 mM L-glutamine, and 0.025% BSA; pH 7.4) for 2 hours at 37°C in air, after which basal respiration was measured. After the assessment of basal respiration, oligomycin (4 µg/mL), carbonyl cyanide-p-trifluoromethoxy-phenylhydrazone (FCCP) (3 µM), and rotenone (1 µM) were added as previously described (*64*). All calculations were done as previously described (*65*).

Animal experiments

Rat models. *Model 1*: Male Wistar rats (Taconic) at 8 weeks of age were put on 45% high-fat diet (HFD; D12451, Research Diets; 45% of calories from fat) and injected with 2.5 mg/kg R-sulforaphane (SFN; LKT laboratories) or vehicle (PBS) 3 times/week. At 15 weeks of age, half of the control rats and half of the SFN-treated rats were put on 60% high-fructose diet (HFrD; Research Diets; 60% of calories from fructose), and the remaining animals were put on 60% HFD (D12492, Research Diets; 60% of calories from fat). After 5 weeks on the new diets, an IPITT and an *i.p.* glucose tolerance test (IPGTT) were performed. For the IPGTT, the rats were injected with 1 g/kg glucose. The rats were euthanized using CO_2, and tissues were extracted. Liver samples were used for microarray analysis.

Model 2: Male Wistar rats (Charles River) at 6 weeks of age were put on 60 % HFD or on control diet (D12450J, Research Diets; 10% of calories from fat). After 11 months on the diets, pre-treatment oral glucose tolerance tests (OGTTs) were performed. The HFD-fed rats were then treated with 5 mg/kg/day SFN or vehicle (PBS) for 14 days. The rats on control diet were injected with vehicle only, serving as references for glucose tolerance. Post-treatment OGTTs were then performed. For the OGTTs, a fixed dose of 1.43 g glucose per rat was given by gavage, corresponding to an average dose of 1.9 g/kg for the rats on HFD and 2.7 g/kg for the rats on ctrl diet.

Model 3: Male Wistar rats (Charles River) at 6 weeks of age were put on 60 % HFrD. After 6 months on the diet, the rats were treated either with 10 mg/kg/day SFN *i.p.* or with 300 mg/kg/day metformin (Sigma-Aldrich) *p.o.* for 9-12 days. After 10 days, the rats were subjected to an OGTT (2 g/kg glucose), and after 9 or 12 days they were subjected to an *i.p.* pyruvate tolerance test (IPPTT) to assess hepatic glucose production.

Mouse models. *Model 1* (Diet-induced diabetic mice): Male C57BL/6J Bom mice (Taconic) at 4 months of age were put on 60% HFD for 10 weeks. They were then treated with 0.5 or 10 mg/kg/day SFN *i.p.* daily for 4 weeks, after which they were subjected to an IPGTT and an IPITT. For the IPGTT, the mice were injected with a fixed dose of 0.033 g glucose per mouse (33% glucose in PBS), corresponding to an average dose of 0.73 g/kg for the mice on HFD (average body weight 45 g) and 1 g/kg for the mice on control diet (average body weight 32 g). The mice were euthanized using CO_2, and tissues were extracted. Liver samples were used for measurement of liver triglyceride content.

For glucose production rate measurements and hyperinsulinemic-euglycemic clamp, we used male C57BL/6J mice (The Jackson laboratory) fed 60% HFD from 6 weeks of age. The mice were treated with SFN (10 mg/kg i.p. daily) for 4 weeks from 14 weeks of age before the experiment.

Model 2 (BSE-treated mice): Male C57BL/6J Bom mice (Taconic) at 7 weeks of age were put on 60% HFD for 4 weeks. They were then treated with 1.34 g/kg/day Broccophane broccoli sprout extract (corresponding to 9.5 mg/kg/day SFN equivalents; see below) or with vehicle (water) *p.o.* daily for 4 weeks, after which they were subjected to an IPGTT. For the IPGTT, the mice were injected with a fixed dose of 0.04 g glucose per mouse (33% glucose in PBS), corresponding to an average dose of 1.04 g/kg (average body weight 38.5 g).

Insulin tolerance test. Animals were fasted for 5 hours in the morning before the test. Rats were injected *i.p.* with 1 IU/kg insulin (Actrapid, NovoNordisk), and mice were injected *i.p.* with 0.5 IU/kg insulin. Blood glucose was measured from the tail vein with a glucose meter (Accu-Check Aviva) before insulin injection and at different time points up to 180 min.

Glucose tolerance test. Animals were fasted for 5 hours in the morning before the test. For the different rat models, slightly different glucose tolerance tests (GTTs) were used (intraperitoneal or oral administration and fixed dose or body weight-based dose of glucose; see the animal models). Blood glucose was measured from the tail vein with a glucose meter at different time points up to 120 or 180 min.

Pyruvate tolerance test. Animals were fasted for 5 hours in the morning before the test. Rats were injected *i.p.* with 0.5 mg/kg sodium pyruvate (Merck). Blood glucose was measured from the tail vein with a glucose meter before pyruvate injection and at different time points up to 120 min.

Liver triglyceride measurements. Pieces of liver (around 100 mg) were pulverized under liquid nitrogen using mortar and pestle. Glass tubes with 2 ml hexane:isopropanol (3:2 + 0,005% butylated hydroxytoluene) were precooled at -20°C to avoid evaporation, then around 20 mg of liver powder was added (mass noted). Duplicates were prepared for each liver sample. The tubes were incubated on an orbital shaker at 600 rpm for 1 hour at room temperature and then centrifuged for 10 min at 2500 x g. Lipid extracts were transferred to new glass tubes and kept under nitrogen gas to reduce volume. The remaining liver residues were washed by adding 1 ml hexane:isopropanol (3:2 + 0,005% butylated hydroxytoluene) and allowed to shake for 10 min at 600 rpm before centrifugation and pooling of the obtained extract with the first extract. This washing was done three times. Lipid extracts were dried under nitrogen gas and redissolved in 100-300 µl isopropanol + 1% Triton X-100. Triglyceride concentrations were measured using the LabAssay Triglyceride kit from Wako.

Gluconeogenesis measurement and hyperinsulinemic-euglycemic clamp. Male C57BL/6J mice fed 60% HFD from 6 weeks of age were treated with SFN (10 mg/kg i.p. daily) for 4 weeks from 14 weeks of age before the experiment. The mice were given a last dose of SFN and fasting was started at 1:00. At 3:00, 2 hours after the commencement of the fast, the mice received an i.p. dose of 100 µl ^2H_2O (99% atom percent ^2H, sterile and pyrogen-free, from Cambridge Isotopes Laboratories), resulting in a deuterium enrichment of ~ 0.5% in body water. After this ^2H_2O dose, the mice were given ad libitum access to water containing 0.5% ^2H_2O in order to maintain the body water deuterium enrichment at ~0.5%.

After a 7-8.5 hour fast, the mice were sedated by an i.p. injection with Hypnorm-Dormicum [a 1:2:1 ratio mix of fentanyl/fluanisone (VetaPharma), water, and midazolam (Roche)] and were kept sedated during the entire experiment by additional i.p. doses of fentanyl/fluanisone. Catheters were inserted in the jugular vein for infusion of solutions and in the carotid artery for blood sampling. All solutions used for infusion were prepared in saline with 0.5% ^2H_2O in order to maintain the body water deuterium enrichment at ~0.5%. A primed constant rate infusion of [6,6-$^2H_2$]glucose (99% atom percent ^2H, sterile and pyrogen-free, from Cambridge Isotopes Laboratories) at 15 µg/min (with 900 µg prime during the first 10 min) was started and continued for 2 hours to reach steady state enrichment of the tracer. At 100 and 120 min, ~25 µl of blood was collected and immediately deproteinized by adding 125 µl of acetone for [6,6-$^2H_2$]glucose enrichment analyses by mass spectrometry. At 120 min, blood was also collected in heparin-coated tubes (Sarstedt) for separation of plasma (centrifugation at 2000 g for 15 at 4°C). Plasma was kept frozen at -80º C until analyzed for deuterium enrichment in body water. Acetone supernatant (centrifugation at 2000 g for 15 at 4°C), which constitutes the glucose fraction, was stored at -20°C for subsequent derivatization to glucose pentaacetate.

Immediately after the 2-hour period of [6,6-$^2H_2$]glucose infusion, a 90-min hyperinsulinemic-euglycemic clamp was started. The infusion rate of [6,6-$^2H_2$]glucose was increased to 30 µg/min, and insulin (Actrapid penfill from Novo Nordisk) was infused at 5 mU/kg/min. Unlabeled glucose (20%) was infused at variable rate to maintain euglycemia at 7 mM. Blood glucose was measured with a glucose meter (Accu-Chek Aviva) and glucose infusion rate adjusted every 10 min. At 70 and 90 min, blood for [6,6-$^2H_2$]glucose enrichment analyses was collected and deproteinized with acetone, and at 90 min blood was also collected for plasma samples.

Analyses: The Isotopic enrichment of [6,6-$^2H_2$]glucose was measured by gas chromatography – mass spectrometry (GCMS) (6890/5973 Agilent Technologies) using the pentaacetate derivative (*66, 67*). The incorporation of deuterium in glucose from ^2H_2O was determined using the average deuterium enrichment in glucose carbons 1, 3, 4, 5, and 6 as previously described (*67, 68*). Briefly, this method (*67, 68*) involves preparation of the pentaacetate derivative of glucose, followed by sample analysis using GCMS in positive chemical ionization mode. Selective ion monitoring of m/z 170/169 is performed to determine the M+1 enrichment of deuterium in the circulating glucose carbons (C-1,3,4,5,6,6) (M is the base mass, 169, representing unlabeled glucose). After subtracting the enrichment of M+1 resulting from the natural abundance, the average enrichment of deuterium on a gluconeogenic carbon is calculated from these M+1 data (*67, 68*). Deuterium enrichment in plasma water was determined by Isotope Ratio Mass Spectrometry (Delta+XL IRMS Thermo Finnigan).

Calculations: All kinetic measurements were performed under steady state conditions. Total plasma glucose appearance rate (glucose Ra) was calculated from the M+2 enrichment of [6,6-$^2H_2$]glucose in plasma using established isotope dilution equations (*66*). Under steady state conditions, it is assumed that the rate of appearance (Ra) of glucose is equal to the rate of disappearance of glucose (Rd).

Rate of glucose production (GPR) (mg/kg/min) = (glucose Ra) – (exogenous glucose infusion)

Fractional gluconeogenesis (gluconeogenesis as a fraction of glucose Ra) was calculated according to Chacko et al. (*67, 68*) as follows:

(GNG % Ra) = [(M+1) (^2H) (m/z 170/169) /6] / E ^2H_2O

where (M+1)(^2H) (m/z 170/169) is the M+1 enrichment of deuterium in glucose measured using m/z 170/169, ‘6’ is the number of ^2H labeling sites on the m/z 170/169 fragment of glucose (the average M+1 enrichment derived from deuterated water), and E ^2H_2O is the deuterium enrichment in plasma water. Rate of gluconeogenesis was calculated as the product of total glucose appearance rate and fractional gluconeogenesis:

Rate of gluconeogenesis (mg/kg/min) = (glucose Ra) × (GNG %)

Total plasma glucose appearance rate (glucose Ra) during clamp reflects whole body insulin-stimulated glucose uptake (glucose disappearance rate, Rd)

Primary hepatocyte isolation and glucose production measurements. Primary mouse hepatocytes (PMHs) were isolated from 12-week-old mice fed a standard diet, by a collagenase perfusion method as previously described (*69*), and cultured in DMEM (3 g/L glucose) supplemented with 10% FBS and antibiotics at 37°C and 5% CO_2. Eight hours after isolation, cells were treated with palmitate (500 µM) in the presence or absence of SFN (3 µM) for 24 hours. For glucose production measurements, PMHs were incubated in Krebs buffer supplemented with lactate (20 mM), pyruvate (2 mM), and forskolin (10 µM) for 45 min. An aliquot of the incubation buffer was collected and mixed with perchloric acid 70% and neutralized by KOH MOPS solution (KOH 2N, MOPS 0.3 M in ultrapure water). Glucose concentration was measured by adding hexokinase and measuring resulting NADH absorbance at 340 nM. Glucose production was calculated by subtracting glucose concentration at 0 min from glucose concentration at 45 min.

Study design of clinical trial

Patients. Patients of Scandinavian ethnicity were recruited using the following inclusion criteria: Type 2 diabetes, defined as diabetes mellitus according to the American Diabetes Association criteria and with an absence of GAD antibodies and no known secondary diabetes; written informed consent; age 35-75 years (participating women had to be postmenopausal); BMI 25-40 kg/m^2 at screening visit; HbA1c 6-10 %, equivalent to 41-86 mmol/mol; currently on diet or metformin treatment.

Exclusion criteria were treatment with insulin, other anti-diabetic treatment given as injections, or any oral anti-diabetic treatment except metformin; fasting blood glucose > 15.0 mmol/L; active liver disease; at screening or at any subsequent visit a level of aspartate aminotransferase (ASAT) or alanine aminotransferase (ALAT) of more than three times the upper limit of the normal range; gastrointestinal ailments which may interfere with the ability to adequately absorb sulforaphane; at screening visit creatinine > 130 µmol/L; coagulation disorder or current anti-coagulant therapy with warfarin, which may be affected by the BSE; diagnosed with a cardiovascular disease or event within 6 months prior to enrolment; systemic glucocorticoid treatment; herbal treatment, defined as food supplement (except multivitamin treatment) with herbal or vegetable extracts that may contain sulforaphane; allergy to broccoli; mental disorder making the patient unable to understand the study information; participation in other clinical trial which may affect the outcome of the present study; any other physical or psychiatric condition or treatment that in the judgment of the investigator makes it difficult to participate in the study.

Participants were divided into groups with well-regulated (HbA1c ≤ 50 mmol/mol) and dysregulated (HbA1c > 50 mmol/mol) T2D, and each group was further divided into non-obese (BMI ≤ 30 kg/m^2) and obese (BMI > 30 kg/m^2) patients.

All included patients except 3 well-regulated participants were treated with metformin (500-3000 mg). No patient reported a change of their dose during the study. Patients were enrolled between Sept 2015 and April 2016. The study was conducted at Skåne University Hospital, Sweden. The study was approved by the regional ethics committee in Lund. All participants gave written informed consent. Data safety monitoring organization was FoU-Centrum, Region Skåne, Sweden.

Design of clinical study. The study was a randomized double-blind placebo-controlled study. Patients attended a screening visit at which basic clinical information and fasting blood samples were collected to check whether the patients matched the study criteria. Approximately 2 weeks later, the patients underwent an OGTT by drinking a water suspension with 75 g glucose. Glucose and insulin were measured at 30, 60, 90, and 120 minutes after the glucose intake. The patients were instructed not to conduct intense physical activity or drink alcohol 24 hours before the visit. They were fasting from midnight. Included patients then received placebo or BSE for 12 weeks.

The study team contacted the patients by phone 2-4 weeks after the initiation of the treatment to check compliance and side effects.

After the 12-week treatment period, the patients returned for a final visit. The patients returned any remaining study compound, and the number of remaining bags was noted. Only patients who have taken >75% of their compound during the total study period and >80% during the last month were included in the analyses. Adverse events were noted and appropriate follow-up initiated. Fasting blood samples were drawn and a final OGTT was conducted.

Glucose was measured immediately in venous whole blood by a Hemocue blood glucose meter. All other blood analyses except dithiocarbamate were done at the central hospital laboratory using enzyme-linked immunosorbent assays, radioimmunoassays, and enzymatic colorimetric method.

Dithiocarbamate levels in patient serum were analyzed by the cyclocondensation reaction for measurement of sulforaphane and its metabolites (*37*).

Study compound. BSE containing high amounts of the sulforaphane precursor glucoraphanin was provided by Lantmännen R&D. BSE was produced by cultivation of seeds from a high sulforaphane-containing broccoli cultivar. The sprouts were then harvested, sterilized, sprouted, and dried before milling. 20 kg of broccoli sprouts yield approximately 1 kg of broccoli extract, a concentration of 20:1.

Maltodextrin sprayed with copper chlorophyllin was used as placebo. BSE was also mixed with a smaller amount of placebo (maltodextrin sprayed with copper-chlorophyllin) to give the active (BSE) and placebo treatment a similar appearance. The placebo doses contained 4 g of powder (64.8 kJ), and the active BSE doses 5 g of powder (83.9 kJ). Sulforaphane content was determined by reverse phase high performance liquid chromatography (HPLC) by Eurofins in Sweden. Briefly, sulforaphane content in the sample was determined after hydrolysis by 25 units of thioglucosidase (myrosinase). The samples were analyzed using a Spherisorb ODS C-18 column with a proprietary gradient program and detection at 240 nm. Quantitation was based on a 3-point linear regression of the response factor of a commercially available sulforaphane standard. The SFN content was 5410 ppm in the active BSE dose, and no SFN was detected in the placebo.

Placebo or BSE powder was provided as dry mixtures in sealed portion size bags. The mixtures were suspended with liquid (for example, water) and were ingested once daily in the morning.

For treatment of H4IIE cells, placebo or BSE was dissolved in water, homogenized with an Omni TH homogenizer, and allowed to stir for 30 min at room temperature. The extract was then sterilized using a 45-μM filter before adding it to the cells. We also prepared an inactive BSE control in which myrosinase and sulforaphane were denatured/degraded by boiling: the BSE powder was added to boiling water and allowed to boil for 5 min before homogenization, stirring, and filter sterilization.

Statistical analysis of patient data. Patients were analyzed using intraindividual one-tailed comparisons before and after treatment. The primary effect variables were HbA1c after vs. before the treatment (ΔHbA1c) and fasting glucose after vs. between the treatment (Δglucose). Secondary variables were BMI, HOMA-IR, insulin sensitivity index (ISI), glucose at 2 hours of the OGTT, a fatty liver index (based on BMI, waist circumference, triglycerides, gamma-glutamyl transferase (*48*)), HOMA-B, and insulinogenic index. All analyses were done using one-tailed Student's t-test to compare between placebo and BSE arms. We also performed two-tailed linear regression to compare the relationship between metabolic variables and ΔHbA1c and Δglucose as described in the text. Patients' compliance was checked, and all 97 patients met our criteria for inclusion in the analysis. Six patients interrupted the study and were not included. Statistical analyses were performed using IBM SPSS Statistics (ver. 20.0) or Excel.

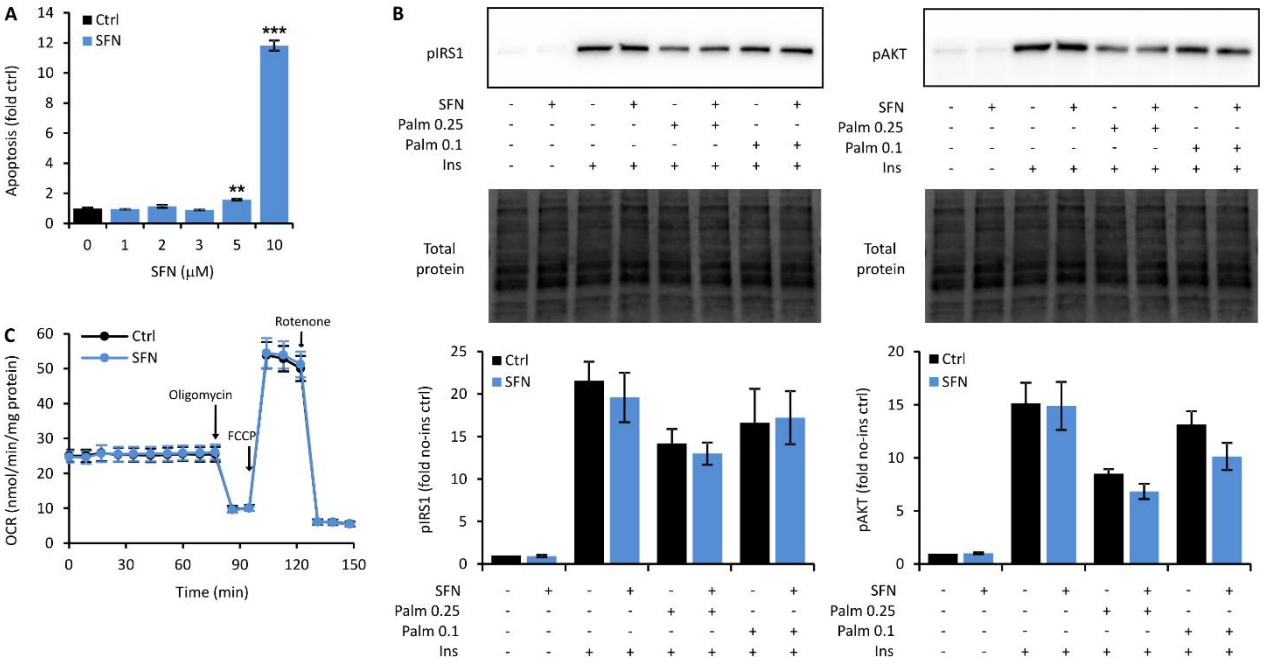

Fig. S1. Effect of SFN on apoptosis, insulin signaling, and OCR in H4IIE cells.

(A) Apoptosis measured by the presence of mono- and oligonucleosomes in the cytoplasm of H4IIE cells incubated with the indicated concentrations of SFN for 24 hours (*n*=3).

(B) Insulin signaling in H4IIE cells measured by the amounts of IRS1 protein phosphorylated at Tyr608 (pIRS1) and AKT phosphorylated at Ser473 (pAKT). Representative immunoblots are shown. The cells were treated with 0.25 mM BSA-bound palmitate (Palm 0.25), 0.1 mM BSA-bound palmitate (Palm 0.1), or BSA ctrl, with or without 3 μM SFN for 48 hours. Cells were harvested after 15 min of stimulation with 10 nM insulin (*n*=3).

(C) Mitochondrial oxygen consumption rate (OCR) measured by Seahorse XF24 in H4IIE cells that had been incubated with 3 μM SFN for 24 hours. A glucose-free buffer containing pyruvate, L-lactate, and L glutamine was used for the measurements. Oligomycin (which inhibits ATP synthase, used to assess the mitochondrial proton leak; 4 μg/ml), the uncoupler FCCP (which maximizes respiration; 3 μM), and rotenone (which inhibits the electron transport chain; 1 μM) were added as indicated (*n*=4).

Data are mean ± SEM. Statistical significance **p<0.01; ***p<0.001

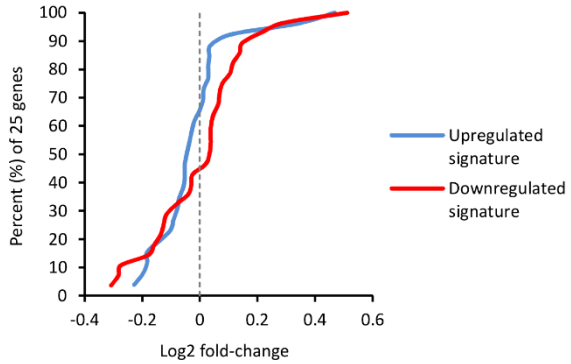

Fig. S2. Effect of SFN on the 50-gene hepatic disease signature.
Cumulative density function plot of the 25 upregulated and the 25 downregulated genes in the hepatic disease signature in liver tissue from rats on 60% HFrD treated with 2.5 mg/kg SFN three times a week for 27 weeks. Gene expression was analyzed by microarray and is expressed as log2-transformed fold-change compared to vehicle-treated rats (*n*=5 animals per group).

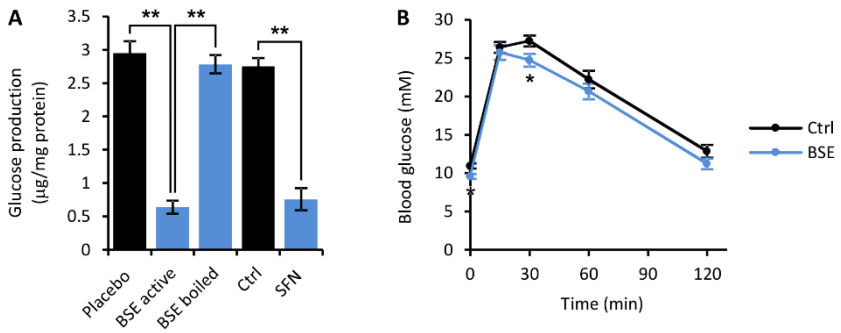

Fig. S3. Effect of BSE on H4IIE cells and on mice fed an HFD.

(A) Glucose production in H4IIE cells after 24 hours of preincubation with placebo, active BSE (3 µM SFN-equivalents), BSE that was boiled to denature myrosinase and degrade SFN, ctrl (untreated cells), or 3 µM SFN (*n*=3).

(B) IPGTT in male C57BL/6J mice fed 60% HFD for 8 weeks and treated with broccoli sprout extract (BSE) for 4 of those weeks (*n*= 9 in each of the groups).

Data are mean ± SEM. Statistical significance *p<0.05; **p<0.01

Table S1. The 50-gene liver disease signature for T2D.

Downregulated genes	**Upregulated genes**
Gene symbol	Gene symbol
YWHAH	*RNU22*
AP2B1	*FOXQ1*
ACTG1	*TERT*
PRCP	*CMTM8*
PRKCA	*TCL1B1*
RTN3	*PCGF5*
RP23-336J1.4	*TCP10A*
TUBA7	*ATF1*
LGALS9	*GRM1*
SLC35C2	*HOXD11*
GLTP	*TUBGCP3*
ARF4	*GM774*
BGN	*PPM1F*
ALG2	*SLC4A1AP*
FKRP	*PPP1R15B*
BUB3	*BRD8*
RP23-20M18.11	*TNRC6A*
GM1079	*PPCDC*
PPP1CA	*ALDH2*
DUSP8	*TMEM57*
MAP3K15	*RXRA*
SLC35E4	*CCT7*
SEC31L1	*RASGEF1C*
UCP2	*RNASE4*
PRDX3	*HNRPUL2*

Table S2. List of compounds used in the analysis (see separate Excel file).

Table S3. Rank order of compounds (see separate Excel file).

Table S4. Expression of enzymes involved in gluconeogenesis.

Gene name	Symbol	Fold-change	P-value
Pyruvate carboxylase	PC	1.17	0.222
Phosphoenolpyruvate carboxykinase 1 (soluble)	PCK1	-3.6	0.0035
Fructose-1,6-bisphosphatase 1	FBP1	-1.87	0.0007
Glucose-6-phosphatase, catalytic subunit	G6PC	-3.21	0.002

H4IIE cells were incubated with 10 µM SFN for 24 hours, and mRNA expression was analyzed by microarray.

Table S5. Adverse effects in patients treated with BSE or placebo for 12 weeks.

Treatment	Adverse effect
BSE	Viral respiratory infection (*n*=10)
	Gastrointestinal problems (*n*=8), including:
	Loose stools during entire treatment period (n=1)
	Loose stools for a few days after treatment start (n=1)
	Flatulence a few hours after intake (n=2)
	Mild intermittent stomach pain (n=2)
	Mild nausea a few hours after intake (n=2)
	Other (*n*=2)[#]
placebo	Viral respiratory infection (*n*=5)
	Gastrointestinal problems (*n*=7), including:
	Loose stools for a few days after treatment start (n=2)
	Flatulence a few hours after intake (n=1)
	Mild intermittent stomach pain (n=1)
	Mild nausea a few hours after intake (n=1)
	Mild diarrhea during entire treatment period (n=1)
	Moderate diarrhea for a few days in the middle of the treatment (n=1)
	Other (*n*=4)[##]

[#] shoulder problem for 2 days, palpitations for 1 day

[##] back pain, foot pain, Achilles tendinitis, chest pain

Table S6. Characteristics of patients discontinuing the study.

Variable	Discontinued	Continued
Sex (% female / male)	33 / 67	25 / 75
Metformin dose (mg/day)	1258 ± 622	1235 ± 633
BMI (kg/m^2)	31.8 ± 3.2	30.4 ± 4.0
Waist circumference (cm)	107 ± 19	104 ± 9
Hip circumference (cm)	111 ± 13	106 ± 8
Plasma glucose (mmol/L)	8.2 ± 1.3	7.7 ± 2.5
HbA1c (mmol/mol)	51.8 ± 10.6	49.7 ± 6.5
Systolic blood pressure (mm Hg)	139 ± 16	140 ± 20
Diastolic blood pressure (mm Hg)	80 ± 9	81 ± 11
Pulse rate (beats/min)	66 ± 12	69 ± 9
Known drug allergy (% subjects)	17%	31%

Data from first visit presented as means ± s.d. or frequency (%) among patients continuing (n=97) and discontinuing the entire study (n=6). There were no significant differences between groups, and we did not observe any systematic differences in concomitant diseases or medication between groups.